Progress in Biophysics and Molecular Biology 115 (2014) 198–212

Contents lists available at ScienceDirect

Progress in Biophysics and Molecular Biology

journal homepage: www.elsevier.com/locate/pbiomolbio

Review

Images as drivers of progress in cardiac computational modelling

Pablo Lamata [a, b, *], Ramón Casero [c], Valentina Carapella [b], Steve A. Niederer [a], Martin J. Bishop [a], Jürgen E. Schneider [d], Peter Kohl [e, b], Vicente Grau [c]

[a] Dept. Biomedical Engineering, Division of Imaging Sciences and Biomedical Engineering, King's College of London, London, United Kingdom
[b] Dept. Computer Science, University of Oxford, Oxford, United Kingdom
[c] Institute of Biomedical Engineering, Department of Engineering Science, University of Oxford, Oxford, United Kingdom
[d] Radcliffe Department of Medicine, Division of Cardiovascular Medicine, University of Oxford, Oxford, United Kingdom
[e] National Heart and Lung Institute, Imperial College, London, United Kingdom

ARTICLE INFO

Article history:
Available online 10 August 2014

Keywords:
Computational cardiac physiology
Medical imaging

ABSTRACT

Computational models have become a fundamental tool in cardiac research. Models are evolving to cover multiple scales and physical mechanisms. They are moving towards mechanistic descriptions of personalised structure and function, including effects of natural variability. These developments are underpinned to a large extent by advances in imaging technologies. This article reviews how novel imaging technologies, or the innovative use and extension of established ones, integrate with computational models and drive novel insights into cardiac biophysics. In terms of structural characterization, we discuss how imaging is allowing a wide range of scales to be considered, from cellular levels to whole organs. We analyse how the evolution from structural to functional imaging is opening new avenues for computational models, and in this respect we review methods for measurement of electrical activity, mechanics and flow. Finally, we consider ways in which combined imaging and modelling research is likely to continue advancing cardiac research, and identify some of the main challenges that remain to be solved.

Contents

* Corresponding author. Dept. Biomedical Engineering, Division of Imaging Sciences and Biomedical Engineering, King's College of London, London, United Kingdom. Tel.: +44 (0) 20 71887188x54383.
E-mail address: Pablo.Lamata@kcl.ac.uk (P. Lamata).

http://dx.doi.org/10.1016/j.pbiomolbio.2014.08.005

1. Introduction

From the first models of single cell electrophysiology (Noble, 1960, 1962) the field of cardiac modelling has experienced remarkable progress. Current models incorporate multi-physics phenomena (Hunter et al., 2003; Kohl and Noble, 2009; Nordsletten et al., 2011), combining electrophysiology (Trayanova, 2011), mechanics (Nash and Hunter, 2000), mechano-electric interactions (Hermeling et al., 2012; Hales et al., 2012), fluid flow (Taylor and Figueroa, 2009) and tissue perfusion (Lee and Smith, 2012). They characterize processes across scales, from nano to macro. Cardiac models increasingly incorporate subject-specific information, from ventricular anatomy to electrical and mechanical material properties (Ranjan et al., 2012; Sermesant et al., 2012; Krishnamurthy et al., 2013; Xi et al., 2013). Having proved their value for advancing our insight into mechanisms of (patho-) physiology (Hunter et al., 2001), models are now moving to applications in the clinic (Burnes et al., 2000; McDowell et al., 2012).

Healthy cardiac function depends on the interplay of multiple biophysical phenomena. The elucidation of mechanisms and their complex interrelations is particularly challenging when using a purely experimental approach. Mechanistic description, quantitative analysis, identification of causal interrelations, consideration of dynamic behaviour, and – in particular – prediction, are domains where computational modelling has started to play a prominent role in cardiac research. In this context, models enable one to integrate and interpret experimental data, to form and test hypotheses about cardiac function, and to assess physiological variables that may not be open to direct measurement due to their invasiveness or for technical reasons (e.g. lack of techniques to measure local stress *in situ*).

Electrophysiologically, cardiac cells can be divided into excitable (mainly cardiomyocytes; note that intra-cardiac neurons are generally excluded from cell-based cardiac modelling) and non-excitable (mainly fibroblasts, endothelial, immune and fat cells). In healthy myocardium, cardiomyocytes occupy ~75% of tissue volume. The remainder is dominated by fibroblasts, accounting for ~60–70% of all cardiac cells (Camelliti et al., 2005). The heart is an organ with built-in pacing and conduction capability, from the sinoatrial node, via the atrio-ventricular node and the specialised Purkinje system, to ventricular cardiomyocytes. The generated electrical wavefront triggers well-coordinated contraction of the muscle. On the cellular level, a wide range of cardiac EP models have been developed for the various cell sub-types involved in this process (e.g. (Zhang et al., 2000; Li and Rudy, 2011; Noble, 2011; Britton et al., 2013)), and the introduction and use of cell-level mark-up languages (like CellML) and associated tools are improving model exchange and re-use (Lloyd et al., 2004; Pitt-Francis et al., 2006; Garny et al., 2009; Gianni et al., 2010; Kerfoot et al., 2013). At the tissue level, cardiac EP models have traditionally considered the myocardial wall as a continuum (Garny et al., 2003; Clayton et al., 2011; Cooper et al., 2011), typically introducing anisotropy through conductivity tensors.

From a mechano-anatomical model perspective, the heart can be decomposed into active and passive components. The mechanically active component is formed by the contractile cardiomyocytes, while the mechanically passive component comprises intra-cellular visco-elastic structures (both in cardiomyocytes and non-myocytes) and the extra-cellular matrix which provides the deformable skeleton of the heart (Weber et al., 1994). Similarly to EP models, cardiac mechanical models traditionally represent this microstructure as a continuum, encoding microstructure in the anisotropy of the contractile and material properties (Hunter et al., 2003). More recent attempts have tried to incorporate the hetero-cellular nature of heart muscle (Xie et al., 2009), and the feedback from mechanical to electrical behaviour of the heart (Kohl et al., 1999, 2006; Li et al., 2004).

From a fluid dynamics perspective, the ventricles are chambers whose inflow and outflow tracks are controlled by valves. Blood can be accurately represented as an incompressible fluid, and inside the cardiac chambers and big vessels its constitutive behaviour can be approximated by a Newtonian model.

Depending on the specific research question addressed, a cardiac model can represent a combination of the aforementioned three physical domains: EP, mechanics and fluidics. The two most common combinations are electro-mechanical (Trayanova, 2011) and fluid–solid interaction models (Taylor and Figueroa, 2009) for the study of the ventricles and main vessels, respectively.

The synergy between experimental methods (e.g. data from images and functional maps) and theory (computational models) is key in the generation of novel insight in cardiovascular science (Quinn and Kohl, 2013). The availability of novel imaging technologies, and the innovative use or extension of established ones, are main drivers of this progress. Recent years have seen dramatic improvements in imaging capabilities, and a rapid expansion of their application. Images cover most of the scales relevant to cardiac modelling, from subcellular structures (Iribe et al., 2009) to whole organs (Pope et al., 2008; Trayanova, 2011). Images have moved from characterizing static structures to providing dynamic measures of function (Townsend, 2008), including electrophysiology, mechanics and blood flow, and modern techniques even probe different aspects of metabolic activity (Taegtmeyer and Dilsizian, 2013). Image analysis methods, allowing the combination of images from multiple subjects, are gradually enabling the transition from individual to population studies (Young and Frangi, 2009).

For these reasons, imaging and modelling are increasingly linked. Development of computational models relies on information acquired from images. Image data have become drivers of progress in cardiac computational modelling in three general areas (Fig. 1). First, they capture **anatomy**, providing the **structural information** necessary to run simulations (MacLeod et al., 2009). Secondly, images provide **functional information** used to build, adjust and validate models (Carusi et al., 2012). When models are not able to reproduce the data contained in images, model limitations are identified, and new mechanisms may be unveiled (Kohl et al., 2010). Thirdly, images are used to estimate model parameters by **data assimilation** (Sermesant et al., 2006b), finding the model parameters that best explain the observed data. These parameters can then be fed back to experimental investigations, or be used as biomarkers. Models also feedback onto imaging methodologies providing a framework for integrating images across multiple scales, for interpreting measurements introducing the biophysics of the system and for linking data across different imaging platforms.

In this review, we concentrate primarily on the scales from tissue to whole organ. Subcellular structures rely on a separate set of imaging technologies (Iribe et al., 2009; Wong et al., 2013) and

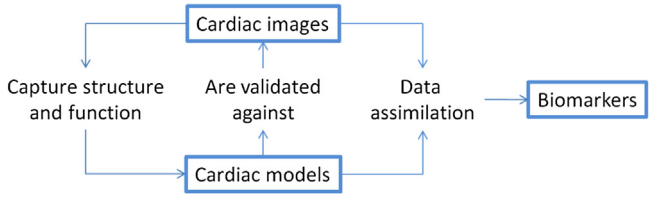

Fig. 1. Conceptual scheme of how cardiac images interact with computational models to generate novel insight and drive research progress.

modelling approaches (Winslow et al., 2006; Gaur and Rudy, 2011), and while there are relevant conceptual similarities, these merit a review on their own. Rather than presenting an exhaustive list of papers, we aim at providing a consideration of the main trends in the field, highlighting in particular how the use of novel imaging technologies is opening up new possibilities for innovation. We illustrate this by offering representative examples covered in previous publications. We do not provide details about modelling, but instead refer the reader to recent reviews and original sources.

Following this introduction, the paper is organized as follows. Section 2 provides an overview of imaging modalities that have become established in clinical cardiac assessment, and of the ways in which they have been applied in combination with computational models. Sections 3 and 4 focus on more experimental imaging techniques, illustrating specific areas in which progress in modelling has been made possible through advances in imaging technologies, and/or in which new imaging developments have been motivated by the needs of modelling research. This is separated into new imaging technologies currently pushing the boundaries of structural (Section 3) and functional (Section 4) characterization of the heart. Section 5 discusses current and future challenges and opportunities involving the combination of images and models in cardiovascular science and medicine.

2. Established clinical imaging technologies: An overview

Imaging has become an integral part of cardiac health and disease assessment. Several cardiac imaging modalities are now widely available in the developed world, and are used as part of standard procedures recommended by the relevant medical societies. As models evolve towards clinical application, data from these imaging modalities are commonly available to build personalised models. Understanding strengths and limitations (including those arising from clinical constraints) of the various techniques is fundamental for successful interrelation with computational modelling. This Section provides an overview of several well-established imaging technologies that have been used in combination with computer models, and discusses representative examples of their application in specific computational modelling studies.

2.1. Echocardiography

Echocardiography often is the first-resort imaging modality in the clinics, due to its low cost (Pennell et al., 2004), lack of ionising radiation, safety, rapid evaluation, easy transportation to the bedside and availability in the operating theatre. Handheld ultrasound systems have become available, providing even higher portability and encouraging routine use in the out-of-hospital setting. Transthoracic echocardiography, the most common echocardiographic investigation, is fully non-invasive, and even invasive transesophageal exams require only mild or no sedation, and involve no incisions. Echocardiographic images show a distinct texture of locally varying signal intensities, commonly referred to as speckle. Speckle tracking can be used to study tissue deformation and thus estimate strain and strain rate. This is useful for the assessment of systolic and diastolic function, and for the identification of regional motion abnormalities indicative of ischemia or scarring (Blessberger and Binder, 2010; Mondillo et al., 2011).

The uptake of echocardiographic data for model development has been limited so far, but insightful case examples exist: e.g. its use in combination with simple mechanical models to identify the contribution of the right ventricle to improved pump function induced by cardiac resynchronization therapy (Lumens et al., 2013), or to evaluate the relevance of different dyssynchrony indexes to predict the response to the same therapy (Lumens et al., 2012), or to predict the improvement in contractile behaviour after cardiac revascularization (Han et al., 2005). Echocardiography has recently benefited from further important advances in technology that will affect the development of computational models and give rise to novel insights. The development of gas-filled microbubbles for use as contrast agents has enabled the evaluation of perfusion (Bhatia and Senior, 2008). In addition, 3D echocardiography increasingly overcomes the limitations of 2D data, albeit generally at a cost of reduced spatio-temporal resolution. 3D echo can also provide data suitable for generation of valid anatomical models of the right ventricle and the cardiac valves (Lang et al., 2012).

2.2. Cardiac Magnetic Resonance Imaging

Cardiac Magnetic Resonance Imaging (MRI) can provide a rich set of data, including information on cardiac anatomy, mechanics, microstructure, perfusion, and other tissue properties. Consequently, MRI has been proposed as a “one-stop-shop” for the analysis of the heart (Poon et al., 2002), and it is considered the gold-standard for assessing cardiac anatomy and function. On the flip side, cardiac MRI is relatively slow, typically involving a combination of acquisitions over several cardiac cycles using the electrocardiogram (ECG) for gating. Long acquisition time also affects resolution, and MRI datasets typically consist of a number of two-dimensional slices acquired at different locations and orientations. MRI can introduce risks to patients with implanted devices which, in turn, can affect the quality of information acquired (Ainslie et al., 2014), though MRI-compatible devices have started to become more generally available (Wilkoff et al., Sommer, 2011).

The possibility of obtaining accurate anatomical and functional information from a single imaging modality, the relatively “clean” appearance of the images (in comparison to echocardiography), and the relatively widespread availability of MRI have led to its use in many cardiac modelling studies, e.g. (Plank et al., 2009; Vadakkumpadan et al., 2009; Conti et al., 2011; Bishop and Plank, 2012; Krishnamurthy et al., 2013), as will be illustrated in more detail in Sections 3 and 4 below.

2.3. Computed Tomography (CT)

Computed Tomography (CT) provides excellent anatomical resolution, both spatial and temporal, but it involves exposure to ionizing radiation. It allows accurate assessment of cardiac functional properties such as left ventricular stroke volume and ejection fraction, and of morphological characteristics such as congenital heart disease, cardiac masses, regional wall motion, presence and location of thrombi, pericardial disease. In addition, CT has recently been proposed for perfusion assessment (Peebles, 2013). The quality and reproducibility of images enables the adoption of robust automatic segmentation solutions for cardiac chambers (Ecabert et al., 2008).

The excellent anatomical detail provided by this imaging modality has enabled detailed computational investigations, such as of the effects of vessel anatomy on blood flow (Taylor and Figueroa, 2009). Personalised models of the coronaries predict an important clinical marker, the flow reserve, without the need of catheterization, constituting an excellent example of successful translation of model-based imaging to clinical practice (Taylor et al., 2013). CT also provides the opportunity to build personalised ventricular models of subjects with implantable devices, such as a left ventricular assisted device, and then optimise the settings of the device by identifying the flow regime that maximises myocardial unloading and homogenisation of work (McCormick et al., 2014).

3. Anatomical model improvements driven by novel imaging techniques

While established imaging modalities will continue playing substantial roles in the development, application and validation of cardiac computational models, continued advances in imaging technologies are pushing the boundaries of model-based cardiac research. Novel technologies allow probing the heart at unprecedented resolution levels, measuring different aspects of cardiac function, and quantifying anatomical and functional variability in health and pathology. In the next two Sections we review specific aspects in which imaging technologies are driving progress in computational models. Section 3 focuses on anatomical characterization, discussing in particular three aspects: (i) the introduction of meso-scale anatomical structures, beyond the standard representation of ventricular and atrial cavities and walls; (ii) moving towards micro-scale, the characterization of cellular structures; and (iii) the quantification of anatomical variability using multi-subject studies and advanced computational statistical atlases.

3.1. Models including meso-scale anatomical structures

While models using simplified geometries have demonstrated their utility in elucidating fundamental mechanisms of cardiac function, a number of studies have shown the importance of finer-scale structures, including papillary muscles (Kim et al., 1999; Bishop et al., 2010b), blood vessels (Luther et al., 2011; Bishop et al., 2012), trabeculations (Bishop et al., 2010b; Sands et al., 2011), and the Purkinje network (Vigmond and Clements, 2007; Ten Tusscher and Panfilov, 2008; Romero et al., 2010; Bordas et al., 2011). Recognition of the importance of small structures, together with advances in computational methods, has motivated the development of high-resolution models. These models are generally made possible by high-resolution structural MRI scans (see Fig. 2), which at present are obtained *ex vivo* in fixed (Bishop et al., 2010b; Vadakkumpadan et al., 2010) or live tissue (Schuster et al., 2012; Hales et al., 2012; Odening et al., 2013).

High resolution *ex vivo* MRI (also referred to as MRI microscopy) has been employed to obtain detailed ventricular geometries in experimental studies (Gurev et al., 2011), and to identify infarcted regions (Vadakkumpadan et al., 2010), leading to computational studies of the electrophysiological effect of the location, size and shape of infarcts. While *ex vivo* MRI microscopy offers the possibility of characterizing small structures, down to voxel sizes in the order of 10^{-8} m (Gilbert et al., 2012), it is limited in several aspects. Excision and fixing of the heart gives rise to deformations, which require nonlinear registration to the *in vivo* geometry for compensation (Plank et al., 2009). *Ex vivo* hearts experience a drift in their properties with time, even after chemical fixation, potentially leading to significant changes in MRI acquisitions (Hales et al., 2011). Fixation in different states of contraction has been demonstrated (Plank et al., 2009), but individual hearts can only be fixed in one state which complicates the analysis of cardiac motion effects in fine scale structures. That said, progress is being made in MRI microscopy of isolated perfused hearts, which are now yielding high-resolution data from multiple deformation states in one and the same sample (see (Hales et al., 2012) and the paper by Lohezic et al., 2014).

Detailed models of ventricular anatomy with high-resolution MRI have provided insights on the efficacy of defibrillation after infarction, finding that the change of properties in the peri-infarct zone explain the increased vulnerability (Rantner et al., 2012), and proposing low-voltage defibrillation protocols to convert ventricular fibrillation into tachycardia, and then terminate tachycardia (Rantner et al., 2013a). Computational modelling studies of the atria have also benefitted from the availability of high-resolution MRI scans, with models being applied to analysing the effects of tissue remodelling, the presence of fibrosis (McDowell et al., 2012, 2013), and the arrangement of endocardial bundles (McDowell et al., 2011; Maesen et al., 2013) in atrial fibrillation.

Electric disorders, such as reentrant arrhythmias, are often closely associated with the presence of heterogeneities in the myocardium, and thus the study of such phenomena requires incorporation and analysis of the impact of finer-scale anatomical details within models. Experimental investigations have demonstrated that distinct anatomical features (such as papillary muscle insertion sites, endocardial trabecular invaginations, or large subepicardial blood vessels) play a potentially important role in stabilising reentrant arrhythmias (Pertsov et al., 1993; Kim et al., 1999; Valderrábano et al., 2001, 2003; Nielsen et al., 2009), providing a substrate which attracts and anchors rotors. Recently, computational models derived from high-resolution MR and containing such levels of finer-scale anatomical detail (Bishop et al., 2010b), have been instrumental in providing a full three-dimensional understanding of these mechanisms (Bishop et al., 2010a; Bishop and Plank, 2012), and the circumstances under which they become important. Furthermore, structural heterogeneity is known to be of great importance during electrotherapy. Both computational bidomain studies (Hooks et al., 2002; Bishop et al., 2010a) and experimental optical mapping measurements (Fast et al., 1998, 2002) have shown how the interaction of conductivity discontinuities, represented by intramural blood vessels and extracellular cleft spaces, may induce 'virtual-electrode' polarisations within the

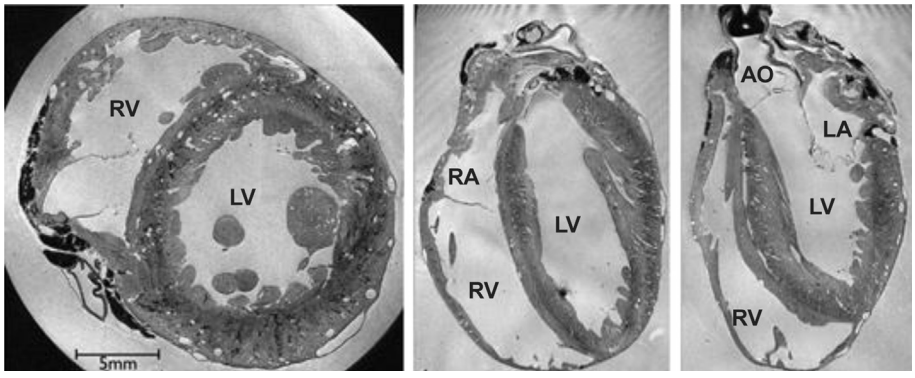

Fig. 2. Sample slices in three orthogonal directions from an *ex vivo* 3D MRI acquisition of a rabbit heart, from Bishop et al. (2010b). The original resolution of the images is 26.4 μm × 26.4 μm × 24.4 μm. LV, RV, LA, RA: Left (right) ventricle (atrium). AO: Aorta.

tissue depth, suggesting this as a mechanism of more effective defibrillation (Luther et al., 2011; Bishop et al., 2012).

3.2. Myocardial microstructure

Our understanding of the spatial organization of myocardial tissue, and its impact on electrical and mechanical function, has greatly improved in recent years. Ventricular myocytes are grouped longitudinally in strands, usually referred to as 'fibres', and laterally arranged in layers, usually called 'sheets'. This arrangement is closely linked to the specific shape of the cardiac myocyte and the extensive collagen network present in cardiac tissue (LeGrice et al., 1995; Spotnitz, 2000; Gilbert et al., 2007). This organization is fundamental for healthy cardiac electro-mechanical function. Of note, both electrical (Kanai and Salama, 1995) and mechanical (Waldman et al., 1988) behaviour are highly anisotropic within ventricular tissue, yet in combination with structurally determined differences in activation timing and stress-strain dynamics, they give rise to externally homogeneous function (as discussed in Solovyova et al. (2006) and by Solovyova et al. 2014).

Microscopy of histological sections has driven knowledge of cardiac cell distribution and morphological interrelations (Spotnitz, 1974), and this data modality remains a gold standard for microstructural tissue characterization. Standard histology techniques, such as the use of trichrome stains to differentiate between myocytes, collagen and other cells (Plank et al., 2009), provide fundamental information about myocardial microstructure. On the other hand, histology has the important shortcoming that processing and mechanical slicing distort the tissue. These non-linear deformations pose significant challenges for 3D tissue reconstruction by alignment of adjacent 2D slices. Estimating cellular orientations in slices has a fundamental limitation also in that angles can only be measured reliably within the cutting plane of a slice. This can be partially compensated by use of non-parallel slices, but since these cannot be extracted from the same location in a single heart, any 3D description based on histology sections is necessarily incomplete. Nonetheless, mathematical models of whole-ventricular fibre distribution, based on histology (Nielsen et al., 1991; LeGrice et al., 1997), have played important roles in cardiac modelling, from early models of cardiac electrophysiology to more recent electro-mechanical ones (Aguado-Sierra et al., 2011; Clayton et al., 2011).

High-resolution confocal microscopy has also been employed to image cell orientation and the 3D arrangement of laminar structures in small samples of myocardial tissue. In contrast to histology slices, confocal microscopy datasets can be obtained in 3D without physical slicing. Current technology is limited, however, to characterisation of small regions that are near the accessible surface, for example to study sarcomere lengths in sub-epicardial tissue in horizontal (Bub et al., 2010) and oblique orientations (Botcherby et al., 2013). Using confocal imaging of embedded tissue, combined with periodic removal of the imaged tissue layers, true 3D reconstruction of cardiac tissue is possible (Pope et al., 2008). Tissue structure distributions, obtained in this way, were introduced in 3D tissue slab electrophysiological simulations (Hooks et al., 2002), demonstrating that not only fibre direction but the anisotropy induced by sheet orientation may affect electrical propagation patterns across the tissue. Confocal imaging has also given further insight into cardiac collagen organisation, including description of extensive meshworks on laminar surfaces, convoluted fibres connecting adjacent layers, and longitudinal cords (Pope et al., 2008).

Diffusion Tensor MRI (DT-MRI) protocols are the state-of-the-art in non-destructive methods to obtain myocyte orientation in cardiac geometries (Sosnovik et al., 2009), initially in fixed hearts as pioneered in (Helm et al., 2005, 2006), but now also applied to *in vivo* human data acquisition, albeit not at microscopic resolution (Nielles-Vallespin et al., 2013). DT-MRI characterizes the diffusivity of water molecules in the myocardium, providing an indirect measure of tissue microstructure, and in particular of the alignment of privileged diffusion spaces in and around myocytes, and the barriers formed by their lateral arrangement into sheets (Scollan et al., 1998). Alternatives to DT-MRI that allow representing complex configurations such as crossing fibres or bifurcations have been proposed (Dierckx et al., 2009) . Direct characterisation of tissue structure in whole hearts is also possible to some extent by high resolution *ex vivo* T2* enhanced MRI (Gilbert et al., 2012).

Models of cardiac electrophysiology based on tissue structure distribution obtained from *ex vivo* DT-MRI acquired from a single subject (Vadakkumpadan et al., 2010), or statistical atlases based on *ex vivo* DT-MRI of multiple datasets (Relan et al., 2011), have been used to predict the evolution of arrhythmia in the infarcted rabbit (Vadakkumpadan et al., 2009) and human heart (Relan et al., 2011).

Given that high-resolution DT-MRI studies are only possible *ex vivo*, solutions have been proposed to build patient-specific fibre models by warping fibre atlases onto patient-specific gross cardiac geometries (McDowell et al., 2013). This approach is also supported by recent results suggesting limited relevance of personalised fibre descriptions for simulation of cardiac mechanics (Carapella et al., 2014). More recently, methods to extract smooth representations of tissue structure distribution from *in vivo* DT-MRI have been developed (Toussaint et al., 2013). This imaging modality has enabled the study of the microstructural regeneration capacity in mice, opening up the possibility of studying the longitudinal effects of interventions such as cell therapy or progression of diseases such as heart failure (Sosnovik et al., 2014).

The combination of realistic geometry from MRI microscopy with realistic tissue structure from DT-MRI is still uncommon, partly because of the high imaging and computational cost associated with both, and with the modelling framework. Simulation of the high-resolution geometry and structure information requires the use of parallel computing approaches and supercomputer facilities (Lafortune et al., 2012). Efforts to exploit this combination have recently started to be undertaken (Gurev et al., 2011; Gil et al., 2013), suggesting that the use of realistic tissue structure distribution will allow electro-mechanical models to predict more realistic global motion and regional strain/stress patterns.

Histology and DT-MRI offer complementary information and their combination can provide rich descriptions of histo-anatomy of the whole heart. Almost a decade ago, a first complete framework to combine histology, high-resolution *ex vivo* MRI, *in vivo* and DT-MRI was presented (Burton et al., 2006). Given the substantial deformations occurring between acquisitions (between *in vivo* and *ex vivo* scans and between MRI and histology), advanced image processing algorithms are required. Additionally, 2D slices need to be combined to produce a 3D representation that can be related to MRI findings, a process that is far from trivial (Gibb et al., 2012). In a related study, the sinoatrial node was reconstructed in human tissue by combined DT-MRI, histology and immuno-histochemistry imaging (Chandler et al., 2011). A similar methodology has been used to build a segmented anatomical and electrophysiological model of the atrioventricular node (Li et al., 2008), and of the sinoatrial node in rabbit (Dobrzynski et al., 2005). A framework to combine high-resolution MRI, DT-MRI and histology has been demonstrated in Plank et al. (2009) to build the most detailed anatomical whole ventricular models to date.

An illustrative example of synergy between imaging and modelling is illustrated by Hales et al. (2012). Computational models of cardiac mechanics typically fail to predict some aspects of cardiac contraction; in particular they tend to underestimate shortening in the apex-base axis, as well as the predominantly centripetal wall thickening. Laminar tissue structure was suggested

as an explanation for this effect in Spotnitz (1974). Confirmation of this basic mechanism, generally missing as an explicit structure from models (changes in sheet angles occurring with contraction), was made possible by DT-MRI studies of individual hearts in two contraction states, using a unique imaging set-up constructed specifically for this purpose (Hales et al., 2012; updated to three mechanical states in the paper by Lohezic et al., 2014).

Atrial walls are much thinner than those of the left venctricle, and their microstructure is mainly characterised by bundles linking atrial sub-structures, and by a thin layer of cells (see recent reviews of atrial modelling in Dössel et al. (2012) and Trayanova (2014)). This microstructure is not well captured by the resolution offered by DT-MRI, but contrast enhanced micro CT has shown to be able to combine an excellent myocyte contrast and voxel resolution, 36 μm (Aslanidi et al., 2013). Realistic 3D atrial tissue models enable a detailed in-silico analysis of electrical disorders, and have recently led to the suggestion of mechanisms that facilitate initiation and maintenance of re-entrant excitation waves (Colman et al., 2013; Trayanova, 2014).

3.3. Analysis of variability

The inclusion of developmental, inter-individual, and disease-related variability in cardiac anatomy and function is an important task area for computational modelling (Britton et al., 2013). Images, and other measurements acquired on individual subjects, provide a subset of the parameters that affect or represent cardiac function. These parameters are usually complemented by standard values or published data acquired in previous studies. A quantitative description of the variability of these parameters is necessary to determine the extent to which the use of standard values affects the validity of model predictions. Estimations of uncertainty can be generated in this process, which may help to select appropriate studies for each specific research question.

Shape variability, for example, can be observed in collections of images, and then quantified through mathematical and statistical tools, including computational atlases. Medical atlases have found wide acceptance in the field of neuroanatomy (Thompson et al., 2000). Similar attempts to capture cardiac structural variability in the form of atlases have been proposed, from gross anatomy Fonseca et al. (2011) to microstructure Lombaert et al. (2012). Initially used as guides for segmentation algorithms (Heimann and Meinzer, 2009), they are now finding their way into computational modelling (Young and Frangi, 2009). Characterization of shape using models has been shown to help quantifying shape bias of imaging protocols (Medrano-Gracia et al., 2013), to allow differentiation of gestational age (Lewandowski et al., 2013), and to be a potential biomarker for adverse cardiovascular events (Lamata et al., 2013a).

4. From anatomy to function

Medical imaging has evolved from the capture of still images, mostly containing anatomical information, to the dynamic characterisation of function. This opens up a range of exciting possibilities in the field of cardiac research, and is arguably the technological area with the potential to produce the strongest driver for conceptual development, in particular through computer modelling.

This section continues the exploration of novel modelling developments, driven by emerging imaging techniques. Here, we focus on image-based characterization of cardiac function, and specifically on three cardiac processes of particular relevance: EP, ventricular wall mechanics, and blood flow inside the cardiac chambers and main vessels.

4.1. Excitation and conduction

Some of the most prevalent and severe cardiac diseases are characterized by EP disorders. The management of these patients requires structure-based information on atrial and ventricular EP, to estimate conduction blocks, re-entry circuits, pro-arrhythmic substrates, etc. General availability of data on cardiac electrical activity has traditionally been limited to the ECG or body surface potential maps. New imaging techniques support acquisition of high-resolution maps of electrical activity *ex vivo* and, with certain limitations, *in vivo*.

Electro-anatomical mapping systems (such as Ensite NaVx from St. Jude Medical, or CARTO from Biosense Webster, see Fig. 3a) have changed the way in which clinicians explore and visualize EP function of patients (Knackstedt et al., 2008; Chubb et al., 2014). These systems combine intra-cardiac catheter tip tracking with field potential recordings, and provide anatomically (relative to the endocardium) resolved EP information *in vivo*. Despite its limited anatomical fidelity, which is further affected by distortions caused by catheter tip interaction with the tissue (in particular in the thin-walled atria), and the difficulty of mapping the EP data to the cardiac anatomy reconstructed from other modalities, electro-

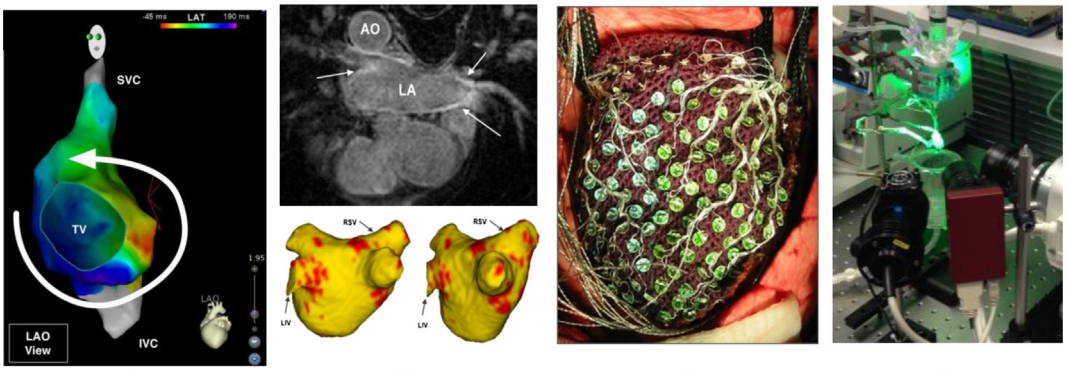

Fig. 3. Imaging techniques to capture cardiac electrophysiological information. (a) Electro-anatomical map of the atrium, obtained by intra-cardiac catheter approaches, showing a re-entry circuit (Chubb et al., 2014; image courtesy of Dr. H. Chubb, KCL); (b) Functional MRI of the heart capturing the extent of fibrosis for ablation therapy of atrial arrhythmias (top), automatically segmented and reconstructed (bottom; Karim et al., 2014; image courtesy of Dr. R. Karim, KCL). AO: Aorta, LA: Left Atrium, RSV: Right Subclavian Vein, LIV: Left Innominate Vein. (c) Multi-electrode cardiac sock for human epicardiac potential mapping (Nash et al. 2006; image courtesy of Dr. M. Nash, University of Auckland); (d) Optical mapping set-up for *ex vivo* Langendorff-perfused rabbit heart (Bishop et al. 2014; image courtesy of Dr. R. Burton and Dr. G. Bub, University of Oxford).

anatomical maps can be used to estimate patient-specific electrical conductivity, and to identify regions of impaired electrical function (Chinchapatnam et al., 2008). Electro-anatomical maps are generated interactively in the catheter lab, and can therefore be used as an on-site guide for ablation procedures (Nademanee et al., 2004). Optimization of pacemakers can also benefit from this modality, since it enables the analysis of intrinsic and paced activation waves (Vatasescu et al., 2009). EP mapping technology also enables simultaneous recordings at several locations through multi-electrode basked catheters; they are generally used for the ventricle, and their non-contact data is less accurate.

EP maps obtained in this way have been adopted into models of the atria (Dössel et al., 2012), which are providing novel insight into atrial fibrosis as a substrate of atrial fibrillation (McDowell et al., 2012), and into models of the susceptibility to arrhythmias of the infarcted heart (McDowell et al., 2011; Karim et al., 2013, 2014). In combination with structural information obtained from other imaging modalities (like late gadolinium enhanced MRI, see Fig. 3b), EP maps have been used to predict risk of arrhythmia recurrence after ablation (Oakes et al., 2009). Access to advanced EP mapping systems is still developing. As they require an invasive procedure, and provide only partial information from extracellular field potentials, EP maps have not yet been widely adopted by the academic modelling community.

The interpretation of EP function measurements is greatly enhanced when combined with specialised structural characterization, facilitated by computational models. Late gadolinium-enhanced (LGE) MRI, also known as delayed enhancement MRI, is an imaging technique that can be used to assess scar location and size after myocardial infarction or ablation (see Fig. 3b). A landmark paper found a correlation between the amount of enhancement and the risk of recurrence after ablation (Oakes et al., 2009), and verified that the regions of greater enhancement were related to regions with low voltage from electroanatomic maps. LGE MRI has gradually been adopted for models of the atria (Dössel et al., 2012), which are providing novel insights about atrial fibrosis as a substrate for atrial fibrillation (McDowell et al., 2012) and the susceptibility to arrhythmia in the infarcted heart (McDowell et al., 2011). Models have successfully predicted ventricular tachycardia circuits (Ng et al., 2012), and suggest a significant potential to reduce ablation procedure time and complication rates by modelling-based pre-procedural planning of optimal ablation targets (Ashikaga et al., 2013). More specifically, models built to investigate tachycardia circuits have found the so-called 'grey zone' to be the arrhythmogenic substrate that promotes re-entry formation (Arevalo et al., 2013).

Multi-electrode cardiac socks record the electrical potential distribution directly from the epicardial surface of the heart. Resultant EP imaging data resolution is much better than in other patient-applicable recording techniques, such as the ECG. Electrode sock recordings have been used intra-operatively in humans (see Fig. 3c). They have been successfully applied to investigate the relevance of the latest activated region for cardiac resynchronisation pacing in the treatment of heart failure (Helm et al., 2007). The combination of EP data from cardiac socks with computational models has supported investigations into heterogeneous restitution properties, and their influence on vulnerability to, and stability of, re-entry in ventricular fibrillation (Nash et al., 2006). Cardiac sock recordings have also revealed differences between animal models and humans in the dynamics of ventricular fibrillation, and computational modelling has been applied to explain these by differences in action potential duration dynamics across species (ten Tusscher et al., 2009). One conclusion that has emerged from these studies is that the simpler spatial organization of human ventricular fibrillation is likely to have important implications for treatment and prevention, highlighting the necessity of combining experimental data and computational models to project between species. Cardiac socks have also been used for simultaneous imaging of endocardial and epicardial electrograms, revealing distinct characteristics of the re-entrant waveforms on each of the surfaces, and thus making a valuable contribution to the understanding of transmural mechanisms of ventricular fibrillation (Massé et al., 2007).

Imaging of EP activity using cardiac socks requires invasive procedures, and data can be substantially affected by artifacts. An alternative is the use of higher resolution surface electrode plaques, which are also invasive but provide finer-scale electrical data (Nademanee et al., 2004; Lee et al., 2014). In addition, transmural EP activity can be acquired through specialised arrays of multi-point recording needles (Valderrábano et al., 2001). These have highlighted, for example, that the so-called M-cells (myocytes with exceedingly long AP durations) would appear to be absent from human myocardium, again referring to the need for careful extrapolation between species (Taggart et al., 2003).

Stretchable electronics (Kim et al., 2011; Chung et al., 2014) constitute a new technology that may allow integration of voltage sensors on conventional balloon catheter membranes, opening up the possibility of high-density measurements with minimally invasive procedures. In a similar way, elastic integumentary membranes, produced via 3D printing to match the shape of the heart, may provide an improved picture of both EP and mechanical response (Xu et al., 2014).

Electrocardiographic imaging (ECGI) – the reconstruction of the electrical activity in the heart from body surface potentials – is a concept with high relevance for the clinical management of patients with cardiac electrophysiological disorders. Mathematically this is an "ill-posed" problem, which can be solved only with the use of appropriate constraints, including an accurate spatial representation of the interrelation of the heart as the electrical source, and the recording locations of mapping electrodes. The feasibility of this approach in humans was demonstrated in a study involved the combination of a vest with 224 electrodes, an accurate anatomical model from CT imaging, and a mathematical solver able to reconstruct electrical potentials, electrograms and isochrones on the heart's surface (Ramanathan et al., 2004). ECGI has since been used to evaluate electrical function in patients from paediatric candidates for cardiac resynchronization therapy (CRT) (Silva et al., 2009) to heart transplant recipients (Desouza et al., 2013), and it has moved to commercialisation (CardioInsight Technologies Inc., Cleveland, USA).

Optical mapping produces images with higher spatial resolution than cardiac socks, using photodetectors to record light emitted by fluorescent dyes that report functional properties (see Fig. 3d). Potentiometric dyes (Laughner et al., 2012) provide an image of trans-membrane voltage changes that can be used to measure activation, action potential duration (and, to some extent, shape), repolarization timing, and conduction velocity. Other fluorescent molecules can be used to measure ion concentrations and dynamics, such as for calcium (Kao et al., 2010). For a review of the state of the art in optical mapping, the reader is referred to (Herron et al., 2012).

Optical mapping has been used to study complex arrhythmias, including fibrillation. In combination with computer models, it has revealed mechanisms that accelerate or stabilize electrical disorders (Noujaim et al., 2007), helped to understand the effect of geometric factors on cardiac vulnerability to electric shocks (Rodríguez et al., 2005), and projected from optical mapping to surface ECG patterns in heart failure (Okada et al., 2011), to name but a few. Optical mapping is limited to acquisition of images that average voltages (or ionic concentrations)

over a certain volume of sub-surface myocardium, and computational models have been critical for their characterization and interpretation (Bishop et al., 2006). There are dynamic differences between optically observed action potentials and the electrical activity in cells such as recorded with microelectrodes, with implications for the interpretation of optical recordings (Bishop et al., 2007). Both optical mapping and multi-electrode contact recordings provide unique data on the dynamics of electrical rotors and spiral waves, and contribute to further understanding of the mechanisms of normal and disturbed sino-atrial node pacemaking (Fedorov et al., 2010), atrio-ventricular conduction (Hucker et al., 2008), and of atrial and ventricular fibrillation (Vaquero et al., 2008) in human. From a model validation perspective, optical mapping has successfully predicted electrical activation waves on alternative pacing configurations (Relan et al., 2011). This has been used to compare cardiac EP models of variable complexities, leading to the proposal to coordinate model parameterization strategies to increase their predictive power (Camara et al., 2011).

In summary, with EP being one of the main targets of cardiac computational methods, the advent of techniques allowing the mapping of electrical activity beyond the standard ECG has been a game-changer in the field. A drawback is that available methods are either limited in spatio-temporal resolution, require invasive procedures, or are applicable to experimental settings only.

4.2. Contraction and relaxation

The concerted interplay of active ejection (systole) and passive relaxation/filling (diastole) of the ventricular chambers is fundamental for effective and efficient pump action of the heart. Management of diseases like heart failure requires accurate methods to characterise myocardial mechanics. Widely available clinical imaging modalities like MRI and ultrasound are used to observe cardiac contraction and relaxation (Ledesma-Carbayo et al., 2005; Brown et al., 2009; Geyer et al., 2010). Image segmentation provides metrics, such as ejection fraction, that can be compared to the clinical setting. Local measurements of strain have the potential to improve patient assessment beyond established global metrics, and they are particularly useful for validating mechanical models.

Considerable efforts have been dedicated to estimating motion from conventional imaging studies like cine MRI, using image registration between frames (see Fig. 4 a–c). Nevertheless, and despite considerable research efforts, image registration algorithms are limited by their assumptions (like the incompressibility of the myocardial walls, which is difficult to ascertain and – in the presence of intra-vascular fluid redistribution - may only be an approximation (Cheng et al., 2005)), the aperture problem (there are several solutions that fulfil the similarity criterion between images), and the possibility of convergence to non-optimal solutions. Cardiac mechanical models have been used to formulate and regularise the problem of image registration, and have thus helped in improving the accuracy and plausibility of the analysis of strain and deformation patterns (Sermesant et al., 2006a). A more accurate alternative is given by the use of motion sensitive MRI scans. Tagged MRI works by superimposing a grid pattern on cardiac MRI intensity; the grid points can then be followed through subsequent time points in the cardiac cycle. This technique has been used for generation and validation of computational models (Bovendeerd et al., 2009; Wang et al., 2009). More recent MRI acquisition protocols (like Diffusion Encoded with Stimulated Echoes [DENSE] or Strain Encoding [SENC] MRI) directly reveal displacement and strain, and reach higher resolution than tagged MRI (Wang and Amini, 2012; Simpson et al., 2013).

Motion measurements can be used for validation in cardiac electromechanical modelling by comparing predicted and observed deformation (Bovendeerd et al., 2009; Wang et al., 2009), or to estimate mechanical material properties of cardiac tissue (Wang et al., 2009; Xi et al., 2011, 2013). These constitutive properties are direct diagnostic biomarkers, and can also be used to personalise computational models for further analysis. However, the estimation of constitutive properties requires simultaneous knowledge of the amount of force (or pressure) that caused a deformation, and the deformation itself (Xi et al., 2014). A further

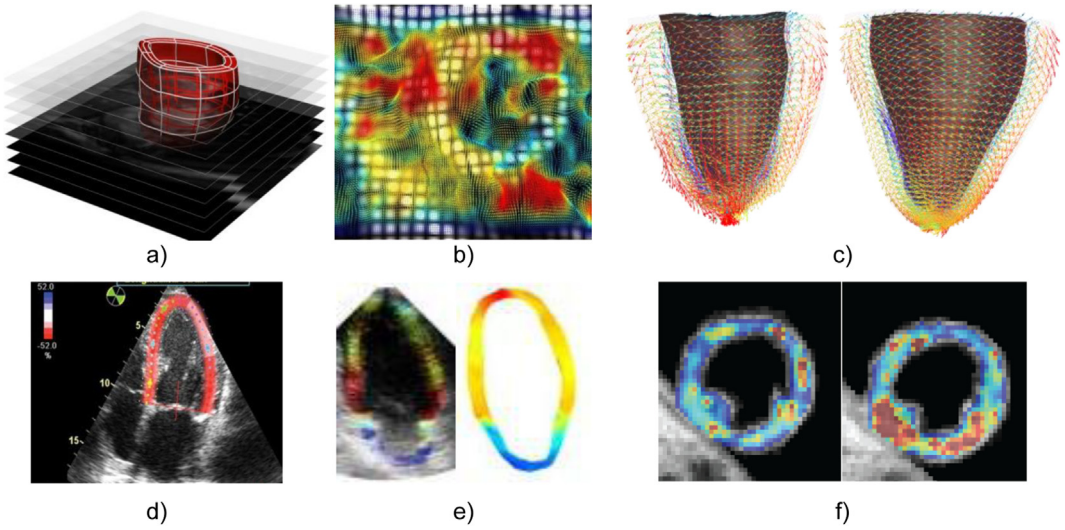

Fig. 4. Illustration of techniques used to capture the mechanical information available in images. (a) Computational mesh of the left ventricle fitted to the domain of the myocardium from the end-diastolic frame of a MRI dynamic short axis stack (Lamata et al., 2011). (b) Tagged MRI frame of a short axis view of the left ventricle with an overlay of a colour encoded deformation field estimated from it by image registration (Chandrashekara et al., 2004). (c) Computational mesh fitted to *in vivo* DT-MRI data (Toussaint et al., 2013) at two instants of the cardiac cycle, systole (left) and diastole (right), with vectors pointing in the direction of the first eigenvector (fibre), colour encoded with respect to the elevation angle (red to blue, +45 to −45). (d) Echocardiographic speckle tracking (Ledesma-Carbayo et al., 2005). (e) Echocardiography-based electromechanical wave imaging (EWI), illustrating the motion maps (left) and the EWI isochrones (right; both colour coded from 0 ms, red, to 300 ms, blue; Provost et al., 2011b). (f) Elastography by the methods described in (Robert et al., 2009): the panel illustrates the shear modulus in a healthy volunteer at two time points of the cardiac cycle (image courtesy of Dr. R. Sinkus, KCL).

challenge arises from the fact that that many cardiac tissue components display visco-elastic behaviour, so that steady state stress-strain relations only provide a partial picture. In turn, non-invasive estimation of central blood pressure, without the need of a catheter, is becoming feasible through recent advances in imaging and modelling. As the acoustic properties of microbubbles change with pressure, this can be captured by echocardiography techniques (Dave et al., 2012). On the other hand, maps of relative pressure can be estimated in theoretical models from flow data (Krittian et al., 2012).

From a modelling perspective, ventricular diastolic behaviour is simpler than systolic, as it is assumed to be dissociated from electrical activity. Contraction, in contrast, strongly depends on the timing of electrical activation. There are two main ventricular factors that influence diastolic ventricular filling, the ability of myocytes to relax after contraction, and the passive compliance (stiffness) of the ventricular wall. Separation of the relative contribution of these two processes has been aided by recent model analysis of MRI sequences (Xi et al., 2013). Extending these methods to the study of contraction will require simultaneous analysis of electrical and mechanical activities, which remains challenging for both imaging and modelling methods.

Among the more recent imaging techniques with interesting potential for computational model development, elastography has been developed to characterise tissue properties *in vivo*. The core concept of this technique is to image deformation, either with MRI (Elgeti and Sack, 2014), see Fig. 4f, or ultrasound (Hollender et al., 2012), in response to a known mechanical stimulus, and to determine the stiffness of the material. The challenge here is the control of the mechanical stimulus (usually a mechanical wave) across the beating and deforming wall of the heart, and the presence of tissue mechanical inhomogeneities at spatial scales that may not be captured by the imaging techniques.

Echocardiographic speckle tracking also captures deformation (see Fig. 4d), but the more commonly used 2D echo images do not lend themselves to mapping 3D mechanics. Nevertheless, speckle tracking can be combined with simplified 2D mechanical models, and this approach has been used to explain different patterns of circumferential strain in heart failure patients requiring CRT (Leenders et al., 2012). Analysis of left ventricular regional wall motion during stress echocardiography has proved to be a useful predictor of coronary artery disease and clinical prognosis, and has in turn been improved by computational models (Herz et al., 2010). Echocardiographic speckle tracking has also been used for validation of predicted deformation patterns for the study of left ventricular torsion (Evangelista et al., 2011).

Another echo-based technique is electromechanical wave imaging (EWI). EWI uses ultrafast echo sequences to capture transient strains in response to electrical activation at high temporal and spatial resolutions, to estimate cardiac activation sequences (Provost et al., 2011b, 2013), see Fig. 4e. The potential utility of EWI in the clinical setting is significant, especially in the context of arrhythmias, including fibrillation, that are associated with extremely fast and potentially lethal changes in cardiac electrical activation and regional motion. The additional ability to locate earliest pacing sites and ischemic regions makes EWI an interesting alternative to ECG mapping, at least for spatial characterisation of electrical activation patterns (Konofagou and Provost, 2012), as electrical and mechanical activation patterns often correlate to an extent that allows deformation-based diagnosis of diseases (Odening et al., 2013). The potential of EWI has only begun to be explored in computational modelling work. EWI patterns have been used to validate a biventricular electromechanical model, reporting good agreement between predicted and measured deformation (Provost et al., 2011a). Given its non-invasive nature and low costs, EWI may be promising for patient-specific modelling that aims to predict the effect of pathologies and/or pharmacological interventions on local electrical and mechanical activation patterns.

An aspect of cardiac mechanics that makes its study particularly suitable for a combined imaging and modelling approach is that fundamental biophysical parameters such as regional stress-strain characteristics are not open to direct experimental exploration, but can be derived from measurement through the use of computational models (Nash and Hunter, 2000). Results obtained in this way can then be fed back to experimental research on isolated cells (Iribe et al., 2007), and also used to investigate the behaviour of cardiomyocytes as mechano-sensors as well as activators (Cooper et al., 2000). This provides an excellent example of an aspect in which imaging and modelling need to work in combination, driving each other's progress.

In summary, in contrast to the limitations in imaging of electrical activity, methods to non-invasively visualize strain with reasonable resolution and accuracy are widely available. However, strain is only part of the picture: mechanical constitutive parameters and stresses (forces, pressure) play fundamental roles in the assessment of cardiac function in health and disease. Computational models have proved useful for this purpose, and their use is likely to play a prominent role in the advance of mechanical characterization methods.

4.3. Ventricular ejection and filling

Characterization of abnormal blood flow patterns and associated key physical parameters, like shear stress, pressure gradients or kinetic energy, are increasingly being adopted for clinical management of diseases like aortic coarctation or valve stenosis (Pedrizzetti et al., 2014).

Doppler ultrasound (see Fig. 5a) captures the blood velocity component parallel to the echo beam, and it is clinically used to assess the severity of obstructions in vessels or the left ventricular outflow track. The pressure gradient is the quantitative metric to characterise obstruction, and its computation typically only requires the peak velocity based on simplistic assumptions (the Bernoulli principle; Gersh et al., 2011). In contrast, computational fluid–solid interaction models can account for the complete mechanics of blood flow, formulated in the Navier–Stokes equations, and be developed from personalised geometries and suitable boundary conditions. These approaches have experienced remarkable progress during the past few years (Taylor and Figueroa, 2009). Prediction of the fractional flow reserve in the coronaries, for example, using geometrical information alone, is a remarkable success in this field (Taylor et al., 2013). The combination of Doppler US with an anatomical modality, MRI, has also enabled the personalization of models to paediatric patients, and the proposal of a metric based on kinetic energy for the assessment of the diastolic function in congenital diseases (de Vecchi et al., 2012).

3D Flow reconstruction is among the more recent imaging-related developments. The reconstruction of dense 3D velocity fields from multiple 3D ultrasound maps is feasible (Gomez et al., 2013), see Fig. 5b. This has the potential of becoming a key tool in computer modelling, providing boundary conditions (i.e. values that can be imposed so the model achieves a realistic prediction) and validating model results. Images of the deformation of the aorta are also commonly available, and it has been demonstrated recently that variations in distensibility along the aorta, and values of pulse wave velocity along the vessel, can be obtained from dynamic sequences of 3D ultrasound maps using image registration regularised by a one-dimensional wave equation (Barber et al., 2014).

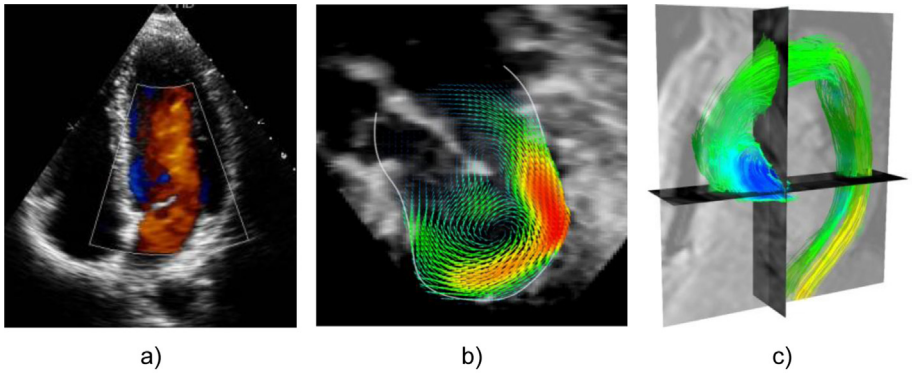

Fig. 5. Illustration of three main imaging technologies used to capture information on blood flow. (a) 2D Doppler echocardiography is widely used in the clinic; (b) 3D flow reconstructed in an infant with mitral stenosis using registration of multiple 3D Doppler acquisitions (Gómez et al., 2013) (c) Phase-contrast MRI, also known as 4D flow data, colour coded by the pressure maps computed from blood flow velocity data (Krittian et al., 2012) in a chronic dissection case.

Phase-Contrast MRI (PC-MRI, see Fig. 5c) provides a spatio-temporal description of blood velocity fields in a 3D domain (Markl et al., 2011). This can be used for the definition of boundary conditions, and for the validation of fluid-solid-interaction models. In a more data-driven approach, PC-MRI has also been used to estimate pressure fields (Krittian et al., 2012) and reveal characteristic patterns that differentiate healthy and diseased subjects (Lamata et al., 2013b), for example using wall shear stress signatures that identify patients with bicuspid aortic valve (Bissell et al., 2013), turbulent (Dyverfeldt et al., 2008) or laminar (Barker et al., 2013) viscous energy loss, etc. Pressure gradients estimated from PC-MRI have also been found to be a suitable surrogate readout (biomarker) to characterise the heart's ability to relax (Yotti et al., 2011).

4.4. *Comprehensive integration of clinical data*

Computational models support integration of different sources of clinical data and images. These can be used to build detailed *in silico* representations of cardiac physiology of individual subjects. Ultimately, this is the basis of personalised medicine, aiming to aid clinical activities from diagnostics to therapy planning. The vision here is that computational models may be used to explore various treatment options, and to tailor interventions to minimize procedure risk while maximizing patient benefit. Availability of patient-specific datasets is becoming a reality in the clinical domain, based on the combination of several imaging modalities, clinical information, and other relevant data (increasingly including genomic data).

An example is the combination of catheter-based electro-anatomical maps and MRI dynamic studies to assess anatomy, tissue deformation and scar location. Personalization of models using this clinical data can aid the management of heart failure patients, specifically the selection for CRT. In this way, the acute response to CRT has been predicted in two patients at different pacing configurations (Sermesant et al., 2012). Models, personalised on the basis of imaging data, have also helped to reveal the role that auto-regulatory mechanisms have in electro-mechanical coupling, and how they affect cardiac responses to CRT (Niederer et al., 2011). These personalised models have contributed to understanding how regional work redistributes in the ventricle after pacing (Niederer et al., 2012a), to identifying that efficient preloading is responsible for a significant stroke work improvement (Hu et al., 2013), and to evaluating the effects of novel pacing leads (Niederer et al., 2012b). Computational models have further been used to analyse abnormal contraction patterns in asynchronous hearts of animal models, and explained these patterns based on well-established electrical and mechanical properties of the myocardium (Kerckhoffs et al., 2008). Models have also recently been used to illustrate how pacing locations can be chosen to optimise both stroke work and ATP consumption (Hu et al., 2014).

5. Discussion: Challenges and opportunities

Recent advances in cardiac structure and function modelling have benefitted from novel imaging modalities and improvements in already established techniques. Enhanced spatio-temporal resolution, an increasing range of functional parameters that can be imaged, and growing signal-to-noise ratios complement anatomical descriptions and increase model utility. The ability to record multiple parameters simultaneously, and to combine different imaging modalities, enriches the information that can be included in conceptual models and quantitative simulations. All this has given rise to substantial developments in the cardiac modelling field.

Mechanisms fundamental to healthy cardiac function cover all scales from the sub-cellular level to the whole organ, and thus computational modelling needs to be multi-scale. In addition to the examples of ‘success stories’ mentioned so far, computational models can help to optimise the placement of implantable cardioverter-defibrillators wires (Rantner et al., 2013b; Rantner et al., 2013b), covering multiple scales from the integration of the full torso, reconstructed from either CT (Jolley et al., 2008) or MRI (Rantner et al., 2013b), to the detailed inclusion of sub-cellular EP mechanisms. An exciting area of development is the prediction at the organ scale of the effects at the level of drug–channel interactions (Moreno et al., 2011), with applications to improving the processes of drug screening (Clancy et al., 2007; Rodriguez et al., 2010; Zemzemi et al., 2013),including inter-species comparisons (O'Hara and Rudy, 2012). Models built from images enable the study of novel concepts, such as the impact of the bioelectric responses to illumination as a potential future mechanism to delivering safe and effective therapy (Boyle et al., 2013).

As models gradually include multi-physics descriptions of the different solid and fluid tissues involved in circulation, we can begin to make use of a broader range of imaging techniques that measure relevant aspects of cardiac physiology. An interesting, yet underutilized in the cardiac field, alternative is based on imaging not the electrical, but the magnetic field generated by the coordinated electrical activation cycle. This technology is used with great success in neurophysiological imaging (magnetoencephalography), and offers excellent temporal resolution and 3D localisation. This can be used to diagnose cardiac rhythm disturbances in particularly

delicate settings, such as before birth *in utero* (Cuneo et al., 2008, 2013).

Despite notable progress towards personalization of models, based on comprehensive sets of available data (Taylor and Figueroa, 2009; Aguado-Sierra et al., 2011; Relan et al., 2011; McDowell et al., 2012; Sermesant et al., 2012; Krishnamurthy et al., 2013; Xi et al., 2013; Lamata et al., 2014), there is a need to improve automation and robustness of underlying processes (Aguado-Sierra et al., 2011), and to find the best compromise between the level of anatomical detail included and the stability of computational meshes and solutions (Lamata et al., 2013c). Research is driven by specific problems, and every study will need to assess the need of model personalization accordingly to the clinical or physiological hypothesis that is to be tested. Subsequently, the need for personalization and the restrictions of each imaging modality will need to be reconciled to determine the optimal imaging protocols (MacLeod et al., 2009).

Improvements in image acquisition techniques must be accompanied by corresponding advances in image analysis. Multi-scale, multi-physics and multi-modal image acquisition calls for novel methods to extract information from large datasets, across different resolutions, and to reliably integrate information from different scans. Fusion of information requires correct spatial and temporal alignment between image data, and careful interrelation with other clinical measurements, such as the ECG or blood pressure measurements, is needed. The integration of image data from different modalities raises the issue of modality robustness and repeatability, particularly in the case of clinical data. The need to balance the use of robust and trusted imaging methods that are 'good enough' to guide current clinical decision making with state-of-the-art ones that may be more prone to application and/or interpretation error needs to be carefully balanced.

Cardiac models are moving from deterministic to stochastic and/or population studies, recognising the importance of natural and pathological variability, from behaviour of individual cells to inter-subject and inter-species variations. Descriptions of standard anatomy and function, as well as their normal and pathological variability, can be condensed in the shape of atlases. These are expected to play an important role in complementing subject-specific data, which are necessarily limited in their resolution and information content. The creation of major repositories of cardiac imaging data (Petersen et al., 2013) could bring substantial rewards in this context. It is fundamental that data as well as methods are shared between groups in public databases. Initial efforts, from The Cardiac Atlas Project (Fonseca et al., 2011) to identification of reporting standards, e.g. MICEE (Quinn et al., 2011), are steps in the right direction, and it will be interesting to see whether they become standard practice in spite of the initial 'extra effort' involved in depositing relevant information.

While perhaps less apparent than the effects that improved imaging methods have had on models, there are also instances in which models have been significant drivers of progress in image acquisition and analysis. Examples include the improved understanding of scattering in optical mapping (Bishop et al., 2007), and the introduction of models in motion estimation techniques to assure that identified motion fields are physiologically feasible (Sermesant et al., 2006a). Synergies and complementarities between imaging and modelling will continue to develop, in particular where a close interaction between the two research fields is achieved. In fact, the majority of commercial imaging systems for clinical use already contains significant image analysis and (albeit somewhat rudimentary) modelling capabilities, that are bound to improve as part of technological progress.

The application of multiple imaging techniques to the same subject can be restricted by time and financial cost, as well as by invasiveness and real or perceived presence of harmful effects associated with individual techniques. In terms of technology development, the challenge ahead is to find optimal combinations of imaging and modelling, suitable to address specific questions in basic and applied research, as well as in the clinic. This will require a mind-set in which the standard sequence of 'modelling follows imaging' is substituted by a combined and interactive development of both, simultaneously.

Editors' note

Please see also related communications in this issue by Prakosa et al. (2014) and Lohezic et al. (2014).

Acknowledgements

Authors thank Professor Natalia Trayanova (Johns Hopkins University) for helpful comments on the manuscript. PL holds a Sir Henry Dale Fellowship funded jointly by the Wellcome Trust and the Royal Society (grant no. 099973/Z/12/Z). JES and PK are British Heart Foundation (BHF) Senior Basic Science Research Fellows (FS/11/50/29038; FS/12/17/29532). RC, VC, JES, PK and VG are supported by the BBSRC BB/I012117/1 and a BHF New Horizon Grant NH/13/30238. PK holds an ERC Advanced Grant (CardioNECT). PL, MJB & SAN acknowledge the support of the National Institute for Health Research Biomedical Research Centre at Guy's and St Thomas' National Health Service Foundation Trust and King's College London and support from the Centre of Excellence in Medical Engineering funded by the Wellcome Trust and EPSRC (Grant WT 088641/Z/09/Z).

References

Aguado-Sierra, J., Krishnamurthy, A., Villongco, C., et al., 2011. Patient-specific modeling of dyssynchronous heart failure: a case study. Prog. Biophys. Mol. Biol. 107, 147–155. http://dx.doi.org/10.1016/j.pbiomolbio.2011.06.014.

Ainslie, M., Miller, C., Brown, B., Schmitt, M., 2014. Cardiac MRI of patients with implanted electrical cardiac devices. Heart 100, 363–369. http://dx.doi.org/10.1136/heartjnl-2013-304324.

Arevalo, H., Plank, G., Helm, P., et al., 2013. Tachycardia in post-infarction hearts: insights from 3D image-based ventricular models. PLoS One 8, e68872. http://dx.doi.org/10.1371/journal.pone.0068872.

Ashikaga, H., Arevalo, H., Vadakkumpadan, F., et al., 2013. Feasibility of image-based simulation to estimate ablation target in human ventricular arrhythmia. Heart Rhythm 10, 1109–1116. http://dx.doi.org/10.1016/j.hrthm.2013.04.015.

Aslanidi, O.V., Nikolaidou, T., Zhao, J., et al., 2013. Application of micro-computed tomography with iodine staining to cardiac imaging, segmentation, and computational model development. IEEE Trans. Med. Imaging 32, 8–17. http://dx.doi.org/10.1109/TMI.2012.2209183.

Barber, D.C., Valverde, I., Shi, Y., et al., 2014. Derivation of aortic distensibility and pulse wave velocity by image registration with a physics-based regularisation term. Int. J. Numer. Method Biomed. Eng. 30, 55–68. http://dx.doi.org/10.1002/cnm.2589.

Barker, A.J., van Ooij, P., Bandi, K., et al., 2013. Viscous energy loss in the presence of abnormal aortic flow. Magn. Reson Med. http://dx.doi.org/10.1002/mrm.24962.

Bhatia, V.K., Senior, R., 2008. Contrast echocardiography: evidence for clinical use. J. Am. Soc. Echocardiogr. 21, 409–416. http://dx.doi.org/10.1016/j.echo.2008.01.018.

Bishop, M.J., Boyle, P.M., Plank, G., et al., 2010a. Modeling the role of the coronary vasculature during external field stimulation. IEEE Trans. Biomed. Eng. 57, 2335–2345. http://dx.doi.org/10.1109/TBME.2010.2051227.

Bishop, M.J., Burton, R.A.B., Kalla, M., et al., 2014. Mechanism of reentry induction by a 9-V battery in rabbit ventricles. Am. J. Physiol. Heart Circ. Physiol. 306, H1041–H1053. http://dx.doi.org/10.1152/ajpheart.00591.2013.

Bishop, M.J., Plank, G., 2012. The role of fine-scale anatomical structure in the dynamics of reentry in computational models of the rabbit ventricles. J. Physiol. 590, 4515–4535. http://dx.doi.org/10.1113/jphysiol.2012.229062.

Bishop, M.J., Plank, G., Burton, R.A.B., et al., 2010b. Development of an anatomically detailed MRI-derived rabbit ventricular model and assessment of its impact on simulations of electrophysiological function. Am. J. Physiol. Heart Circ. Physiol. 298, H699–H718. http://dx.doi.org/10.1152/ajpheart.00606.2009.

Bishop, M.J., Plank, G., Vigmond, E., 2012. Investigating the role of the coronary vasculature in the mechanisms of defibrillation. Circ. Arrhythm. Electrophysiol. 5, 210–219. http://dx.doi.org/10.1161/CIRCEP.111.965095.

Bishop, M.J., Rodriguez, B., Eason, J., et al., 2006. Synthesis of voltage-sensitive optical signals: application to panoramic optical mapping. Biophys. J. 90, 2938–2945. http://dx.doi.org/10.1529/biophysj.105.076505.

Bishop, M.J., Rodriguez, B., Qu, F., et al., 2007. The role of photon scattering in optical signal distortion during arrhythmia and defibrillation. Biophys. J. 93, 3714–3726. http://dx.doi.org/10.1529/biophysj.107.110981.

Bissell, M.M., Hess, A.T., Biasiolli, L., et al., 2013. Aortic dilation in bicuspid aortic valve disease: flow pattern is a major contributor and differs with valve fusion type. Circ. Cardiovasc Imaging 6, 499–507. http://dx.doi.org/10.1161/CIRCIMAGING.113.000528.

Blessberger, H., Binder, T., 2010. Non-invasive imaging: two dimensional speckle tracking echocardiography: basic principles. Heart 96, 716–722. http://dx.doi.org/10.1136/hrt.2007.141002.

Bordas, R., Gillow, K., Lou, Q., et al., 2011. Rabbit-specific ventricular model of cardiac electrophysiological function including specialized conduction system. Prog. Biophys. Mol. Biol. 107, 90–100. http://dx.doi.org/10.1016/j.pbiomolbio.2011.05.002.

Botcherby, E.J., Corbett, A., Burton, R.A.B., et al., 2013. Fast measurement of sarcomere length and cell orientation in Langendorff-perfused hearts using remote focusing microscopy. Circ. Res. 113, 863–870. http://dx.doi.org/10.1161/CIRCRESAHA.113.301704.

Bovendeerd, P.H.M., Kroon, W., Delhaas, T., 2009. Determinants of left ventricular shear strain. Am. J. Physiol. Heart Circ. Physiol. 297, H1058–H1068. http://dx.doi.org/10.1152/ajpheart.01334.2008.

Boyle, P.M., Williams, J.C., Ambrosi, C.M., et al., 2013. A comprehensive multiscale framework for simulating optogenetics in the heart. Nat. Commun. 4, 2370. http://dx.doi.org/10.1038/ncomms3370.

Britton, O.J., Bueno-Orovio, A., Van Ammel, K., et al., 2013. Experimentally calibrated population of models predicts and explains intersubject variability in cardiac cellular electrophysiology. Proc. Natl. Acad. Sci. U. S. A. 110, E2098–E2105. http://dx.doi.org/10.1073/pnas.1304382110.

Brown, J., Jenkins, C., Marwick, T.H., 2009. Use of myocardial strain to assess global left ventricular function: a comparison with cardiac magnetic resonance and 3-dimensional echocardiography. Am. Heart J. 157, 102.e1-5. http://dx.doi.org/10.1016/j.ahj.2008.08.032.

Bub, G., Camelliti, P., Bollensdorff, C., et al., 2010. Measurement and analysis of sarcomere length in rat cardiomyocytes in situ and in vitro. Am. J. Physiol. Heart Circ. Physiol. 298, H1616–H1625. http://dx.doi.org/10.1152/ajpheart.00481.2009.

Burnes, J.E., Taccardi, B., MacLeod, R.S., Rudy, Y., 2000. Noninvasive ECG imaging of electrophysiologically abnormal substrates in infarcted Hearts: a model study. Circulation 101, 533–540. http://dx.doi.org/10.1161/01.CIR.101.5.533.

Burton, R.A.B., Plank, G., Schneider, J.E., et al., 2006. Three-dimensional models of individual cardiac histoanatomy: tools and challenges. Ann. N. Y. Acad. Sci. 1080, 301–319. http://dx.doi.org/10.1196/annals.1380.023.

Camara, O., Sermesant, M., Lamata, P., et al., 2011. Inter-model consistency and complementarity: learning from ex-vivo imaging and electrophysiological data towards an integrated understanding of cardiac physiology. Prog. Biophys. Mol. Biol. 107, 122–133. http://dx.doi.org/10.1016/j.pbiomolbio.2011.07.007.

Camelliti, P., Borg, T.K., Kohl, P., 2005. Structural and functional characterisation of cardiac fibroblasts. Cardiovasc. Res. 65, 40–51. http://dx.doi.org/10.1016/j.cardiores.2004.08.020.

Carapella, V., Bordas, R., Pathmanathan, P., et al., 2014. Quantitative study of the effect of tissue microstructure on contraction in a computational model of rat left ventricle. PLoS One 9, e92792. http://dx.doi.org/10.1371/journal.pone.0092792.

Carusi, A., Burrage, K., Rodríguez, B., 2012. Bridging experiments, models and simulations: an integrative approach to validation in computational cardiac electrophysiology. Am. J. Physiol. Heart Circ. Physiol. 303, H144–H155. http://dx.doi.org/10.1152/ajpheart.01151.2011.

Chandler, N., Aslanidi, O., Buckley, D., et al., 2011. Computer three-dimensional anatomical reconstruction of the human sinus node and a novel paranodal area. Anat. Rec. 294, 970–979. http://dx.doi.org/10.1002/ar.21379.

Chandrashekara, R., Mohiaddin, R.H., Rueckert, D., 2004. Analysis of 3-D myocardial motion in tagged MR images using nonrigid image registration. IEEE Trans. Med. Imaging 23, 1245–1250. http://dx.doi.org/10.1109/TMI.2004.834607.

Cheng, A., Langer, F., Rodriguez, F., et al., 2005. Transmural cardiac strains in the lateral wall of the ovine left ventricle. Am. J. Physiol. Heart Circ. Physiol. 288, H1546–H1556. http://dx.doi.org/10.1152/ajpheart.00716.2004.

Chinchapatnam, P., Rhode, K.S., Ginks, M., et al., 2008. Model-based imaging of cardiac apparent conductivity and local conduction velocity for diagnosis and planning of therapy. IEEE Trans. Med. Imaging 27, 1631–1642. http://dx.doi.org/10.1109/TMI.2008.2004644.

Chubb, H., Williams, S.E., Wright, M., et al., 2014. Tachyarrhythmias and catheter ablation in adult congenital heart disease. Expert Rev. Cardiovasc Ther. 12, 751–770. http://dx.doi.org/10.1586/14779072.2014.914434.

Chung, H.-J., Sulkin, M.S., Kim, J.-S., et al., 2014. Sensors: stretchable, multiplexed pH sensors with demonstrations on rabbit and human hearts undergoing ischemia (Adv. healthcare mater. 1/2014). Adv. Healthc. Mater. 3, 2. http://dx.doi.org/10.1002/adhm.201470002.

Clancy, C.E., Zhu, Z.I., Rudy, Y., 2007. Pharmacogenetics and anti-arrhythmic drug therapy: a theoretical investigation. Am. J. Physiol. Heart Circ. Physiol. 292, H66–H75. http://dx.doi.org/10.1152/ajpheart.00312.2006.

Clayton, R.H., Bernus, O., Cherry, E.M., et al., 2011. Models of cardiac tissue electrophysiology: progress, challenges and open questions. Prog. Biophys. Mol. Biol. 104, 22–48. http://dx.doi.org/10.1016/j.pbiomolbio.2010.05.008.

Colman, M.A., Aslanidi, O.V., Kharche, S., et al., 2013. Pro-arrhythmogenic effects of atrial fibrillation-induced electrical remodelling: insights from the three-dimensional virtual human atria. J. Physiol. 591, 4249–4272. http://dx.doi.org/10.1113/jphysiol.2013.254987.

Conti, C.A., Votta, E., Corsi, C., et al., 2011. Left ventricular modelling: a quantitative functional assessment tool based on cardiac magnetic resonance imaging. Interface Focus 1, 384–395. http://dx.doi.org/10.1098/rsfs.2010.0029.

Cooper, J., Corrias, A., Gavaghan, D., Noble, D., 2011. Considerations for the use of cellular electrophysiology models within cardiac tissue simulations. Prog. Biophys. Mol. Biol. 107, 74–80. http://dx.doi.org/10.1016/j.pbiomolbio.2011.06.002.

Cooper, P.J., Lei, M., Cheng, L.X., Kohl, P., 2000. Selected contribution: axial stretch increases spontaneous pacemaker activity in rabbit isolated sinoatrial node cells. J. Appl. Physiol. 89, 2099–2104.

Cuneo, B.F., Strasburger, J.F., Wakai, R.T., 2008. Magnetocardiography in the evaluation of fetuses at risk for sudden cardiac death before birth. J. Electrocardiol. 41, 116.e1-6. http://dx.doi.org/10.1016/j.jelectrocard.2007.12.010.

Cuneo, B.F., Strasburger, J.F., Yu, S., et al., 2013. In utero diagnosis of long QT syndrome by magnetocardiography. Circulation 128, 2183–2191. http://dx.doi.org/10.1161/CIRCULATIONAHA.113.004840.

Dave, J.K., Halldorsdottir, V.G., Eisenbrey, J.R., et al., 2012. Noninvasive LV pressure estimation using subharmonic emissions from microbubbles. JACC Cardiovasc Imaging 5, 87–92. http://dx.doi.org/10.1016/j.jcmg.2011.08.017.

De Vecchi, A., Nordsletten, D.A., Remme, E.W., et al., 2012. Inflow typology and ventricular geometry determine efficiency of filling in the hypoplastic left heart. Ann. Thorac. Surg. 94, 1562–1569. http://dx.doi.org/10.1016/j.athoracsur.2012.05.122.

Desouza, K.A., Joseph, S.M., Cuculich, P.S., et al., 2013. Noninvasive mapping of ventricular activation in patients with transplanted hearts. J. Electrocardiol. 46, 698–701. http://dx.doi.org/10.1016/j.jelectrocard.2013.05.005.

Dierckx, H., Benson, A.P., Gilbert, S.H., et al., 2009. Intra-voxel fibre structure of the left ventricular free wall and posterior left-right ventricular insertion site in canine myocardium using Q-Ball imaging. In: Ayache, N., Delingette, H., Sermesant, M. (Eds.), Funct. Imaging Model. Hear. Proc. 5th Int. Conf. FIMH 2009, Nice, Fr. June 3–5, 2009. Springer Berlin Heidelberg, pp. 495–504.

Dobrzynski, H., Li, J., Tellez, J., et al., 2005. Computer three-dimensional reconstruction of the sinoatrial node. Circulation 111, 846–854. http://dx.doi.org/10.1161/01.CIR.0000152100.04087.DB.

Dössel, O., Krueger, M.W., Weber, F.M., et al., 2012. Computational modeling of the human atrial anatomy and electrophysiology. Med. Biol. Eng. Comput 50, 773–799. http://dx.doi.org/10.1007/s11517-012-0924-6.

Dyverfeldt, P., Kvitting, J.-P.E., Sigfridsson, A., et al., 2008. Assessment of fluctuating velocities in disturbed cardiovascular blood flow: in vivo feasibility of generalized phase-contrast MRI. J. Magn. Reson. Imaging 28, 655–663. http://dx.doi.org/10.1002/jmri.21475.

Ecabert, O., Peters, J., Schramm, H., et al., 2008. Automatic model-based segmentation of the heart in CT images. IEEE Trans. Med. Imaging 27, 1189–1201. http://dx.doi.org/10.1109/TMI.2008.918330.

Elgeti, T., Sack, I., 2014. Magnetic resonance elastography of the heart. Curr. Cardiovasc Imaging Rep. 7, 9247. http://dx.doi.org/10.1007/s12410-013-9247-8.

Evangelista, A., Nardinocchi, P., Puddu, P.E., et al., 2011. Torsion of the human left ventricle: experimental analysis and computational modeling. Prog. Biophys. Mol. Biol. 107, 112–121. http://dx.doi.org/10.1016/j.pbiomolbio.2011.07.008.

Fast, V.G., Rohr, S., Gillis, A.M., Kléber, A.G., 1998. Activation of cardiac tissue by extracellular electrical shocks: formation of “secondary sources” at intercellular clefts in monolayers of cultured myocytes. Circ. Res. 82, 375–385.

Fast, V.G., Sharifov, O.F., Cheek, E.R., et al., 2002. Intramural virtual electrodes during defibrillation shocks in left ventricular wall assessed by optical mapping of membrane potential. Circulation 106, 1007–1014.

Fedorov, V.V., Glukhov, A.V., Chang, R., et al., 2010. Optical mapping of the isolated coronary-perfused human sinus node. J. Am. Coll. Cardiol. 56, 1386–1394. http://dx.doi.org/10.1016/j.jacc.2010.03.098.

Fonseca, C.G., Backhaus, M., Bluemke, D.A., et al., 2011. The Cardiac Atlas Project—an imaging database for computational modeling and statistical atlases of the heart. Bioinformatics 27, 2288–2295. http://dx.doi.org/10.1093/bioinformatics/btr360.

Garny, A., Kohl, P., Hunter, P.J., et al., 2003. One-dimensional rabbit sinoatrial node models: benefits and limitations. J. Cardiovasc. Electrophysiol. 14, S121–S132.

Garny, A., Noble, D., Hunter, P.J., Kohl, P., 2009. CELLULAR OPEN RESOURCE (COR): current status and future directions. Philos. Trans. A Math. Phys. Eng. Sci. 367, 1885–1905. http://dx.doi.org/10.1098/rsta.2008.0289.

Gaur, N., Rudy, Y., 2011. Multiscale modeling of calcium cycling in cardiac ventricular myocyte: macroscopic consequences of microscopic dyadic function. Biophys. J. 100, 2904–2912. http://dx.doi.org/10.1016/j.bpj.2011.05.031.

Gersh, B.J., Maron, B.J., Bonow, R.O., et al., 2011. 2011 ACCF/AHA guideline for the diagnosis and treatment of hypertrophic cardiomyopathy: a report of the American College of Cardiology Foundation/American Heart Association Task Force on Practice Guidelines. Circulation 124, e783–831. http://dx.doi.org/10.1161/CIR.0b013e318223e2bd.

Geyer, H., Caracciolo, G., Abe, H., et al., 2010. Assessment of myocardial mechanics using speckle tracking echocardiography: fundamentals and clinical applications. J. Am. Soc. Echocardiogr. 23, 351–369. http://dx.doi.org/10.1016/j.echo.2010.02.015 quiz 453–5.

Gianni, D., McKeever, S., Yu, T., et al., 2010. Sharing and reusing cardiovascular anatomical models over the Web: a step towards the implementation of the virtual physiological human project. Philos. Trans. A Math. Phys. Eng. Sci. 368, 3039–3056. http://dx.doi.org/10.1098/rsta.2010.0025.

Gibb, M., Burton, R.A.B., Bollensdorff, C., et al., 2012. Resolving the three-dimensional histology of the heart. In: Gilbert, D., Heiner, M. (Eds.), Comput. Methods Syst. Biol. Springer Berlin Heidelberg, pp. 2–16.
Gil, D., Borràs, A., Aris, R., et al., 2013. What a Difference in Biomechanics Cardiac Fiber Makes. Stat. Atlases Comput. Model. Hear. Imaging Model. Challenges. Springer Berlin Heidelberg, pp. 253–260.
Gilbert, S.H., Benoist, D., Benson, A.P., et al., 2012. Visualization and quantification of whole rat heart laminar structure using high-spatial resolution contrast-enhanced MRI. Am. J. Physiol. Heart Circ. Physiol. 302, H287–H298. http://dx.doi.org/10.1152/ajpheart.00824.2011.
Gilbert, S.H., Benson, A.P., Li, P., Holden, A.V., 2007. Regional localisation of left ventricular sheet structure: integration with current models of cardiac fibre, sheet and band structure. Eur. J. Cardiothorac. Surg. 32, 231–249. http://dx.doi.org/10.1016/j.ejcts.2007.03.032.
Gómez, A., de Vecchi, A., Pushparajah, K., et al., 2013. 3D intraventricular flow mapping from colour Doppler images and wall motion. Med. Image Comput Comput Assist. Interv. 16, 476–483.
Gomez, A., Pushparajah, K., Simpson, J.M., et al., 2013. A sensitivity analysis on 3D velocity reconstruction from multiple registered echo Doppler views. Med. Image Anal. 17, 616–631. http://dx.doi.org/10.1016/j.media.2013.04.002.
Gurev, V., Lee, T., Constantino, J., et al., 2011. Models of cardiac electromechanics based on individual hearts imaging data: image-based electromechanical models of the heart. Biomech. Model Mechanobiol. 10, 295–306. http://dx.doi.org/10.1007/s10237-010-0235-5.
Hales, P.W., Burton, R.A.B., Bollensdorff, C., et al., 2011. Progressive changes in T_1, T_2 and left-ventricular histo-architecture in the fixed and embedded rat heart. NMR Biomed. 24, 836–843. http://dx.doi.org/10.1002/nbm.1629.
Hales, P.W., Schneider, J.E., Burton, R.A.B., et al., 2012. Histo-anatomical structure of the living isolated rat heart in two contraction states assessed by diffusion tensor MRI. Prog. Biophys. Mol. Biol. 110, 319–330. http://dx.doi.org/10.1016/j.pbiomolbio.2012.07.014.
Han, H.-C., Martin, R.P., Lerakis, G., Lerakis, S., 2005. Prediction of the left ventricular ejection fraction improvement using echocardiography and mechanical modeling. J. Am. Soc. Echocardiogr. 18, 718–721. http://dx.doi.org/10.1016/j.echo.2004.12.020.
Heimann, T., Meinzer, H.-P., 2009. Statistical shape models for 3D medical image segmentation: a review. Med. Image Anal. 13, 543–563. http://dx.doi.org/10.1016/j.media.2009.05.004.
Helm, P.A., Tseng, H.-J., Younes, L., et al., 2005. Ex vivo 3D diffusion tensor imaging and quantification of cardiac laminar structure. Magn. Reson Med. 54, 850–859. http://dx.doi.org/10.1002/mrm.20622.
Helm, P.A., Younes, L., Beg, M.F., et al., 2006. Evidence of structural remodeling in the dyssynchronous failing heart. Circ. Res. 98, 125–132. http://dx.doi.org/10.1161/01.RES.0000199396.30688.eb.
Helm, R.H., Byrne, M., Helm, P.A., et al., 2007. Three-dimensional mapping of optimal left ventricular pacing site for cardiac resynchronization. Circulation 115, 953–961. http://dx.doi.org/10.1161/CIRCULATIONAHA.106.643718.
Hermeling, E., Delhaas, T., Prinzen, F.W., Kuijpers, N.H.L., 2012. Mechano-electrical feedback explains T-wave morphology and optimizes cardiac pump function: insight from a multi-scale model. Prog. Biophys. Mol. Biol. 110, 359–371. http://dx.doi.org/10.1016/j.pbiomolbio.2012.07.008.
Herron, T.J., Lee, P., Jalife, J., 2012. Optical imaging of voltage and calcium in cardiac cells & tissues. Circ. Res. 110, 609–623. http://dx.doi.org/10.1161/CIRCRESAHA.111.247494.
Herz, S.L., Hasegawa, T., Makaryus, A.N., et al., 2010. Quantitative three-dimensional wall motion analysis predicts ischemic region size and location. Ann. Biomed. Eng. 38, 1367–1376. http://dx.doi.org/10.1007/s10439-009-9880-1.
Hollender, P.J., Wolf, P.D., Goswami, R., Trahey, G.E., 2012. Intracardiac echocardiography measurement of dynamic myocardial stiffness with shear wave velocimetry. Ultrasound Med. Biol. 38, 1271–1283. http://dx.doi.org/10.1016/j.ultrasmedbio.2012.02.028.
Hooks, D.A., Tomlinson, K.A., Marsden, S.G., et al., 2002. Cardiac microstructure: implications for electrical propagation and defibrillation in the heart. Circ. Res. 91, 331–338.
Hu, Y., Gurev, V., Constantino, J., Trayanova, N., 2013. Efficient preloading of the ventricles by a properly timed atrial contraction underlies stroke work improvement in the acute response to cardiac resynchronization therapy. Heart Rhythm 10, 1800–1806.
Hu, Y., Gurev, V., Constantino, J., Trayanova, N., 2014. Optimizing cardiac resynchronization therapy to minimize ATP consumption heterogeneity throughout the left ventricle: a simulation analysis using a canine heart failure model. Heart Rhythm 11, 1063–1069.
Hucker, W.J., Fedorov, V.V., Foyil, K.V., et al., 2008. Images in cardiovascular medicine. optical mapping of the human atrioventricular junction. Circulation 117, 1474–1477. http://dx.doi.org/10.1161/CIRCULATIONAHA.107.733147.
Hunter, P.J., Kohl, P., Noble, D., 2001. Integrative models of the heart: achievements and limitations. Philos. Trans. R. Soc. A Math. Phys. Eng. Sci. 359, 1049–1054. http://dx.doi.org/10.1098/rsta.2001.0816.
Hunter, P.J., Pullan, A.J., Smaill, B.H., 2003. Modeling total heart function. Annu. Rev. Biomed. Eng. 5, 147–177. http://dx.doi.org/10.1146/annurev.bioeng.5.040202.121537.
Iribe, G., Helmes, M., Kohl, P., 2007. Force-length relations in isolated intact cardiomyocytes subjected to dynamic changes in mechanical load. Am. J. Physiol. Heart Circ. Physiol. 292, H1487–H1497.
Iribe, G., Ward, C.W., Camelliti, P., et al., 2009. Axial stretch of rat single ventricular cardiomyocytes causes an acute and transient increase in Ca2+ spark rate. Circ. Res. 104, 787–795.
Jolley, M., Stinstra, J., Pieper, S., et al., 2008. A computer modeling tool for comparing novel ICD electrode orientations in children and adults. Heart Rhythm 5, 565–572.
Kanai, A., Salama, G., 1995. Optical mapping reveals that repolarization spreads anisotropically and is guided by fiber orientation in guinea pig hearts. Circ. Res. 77, 784–802.
Kao, J.P.Y., Li, G., Auston, D.A., 2010. Practical aspects of measuring intracellular calcium signals with fluorescent indicators. Methods Cell. Biol. 99, 113–152. http://dx.doi.org/10.1016/B978-0-12-374841-6.00005-0.
Karim, R., Arujuna, A., Housden, R.J., et al., 2014. A method to standardize quantification of left atrial scar from delayed-enhancement MR images. IEEE J. Transl. Eng. Heal Med. 2, 1–15. http://dx.doi.org/10.1109/JTEHM.2014.2312191.
Karim, R., Housden, R.J., Balasubramaniam, M., et al., 2013. Evaluation of current algorithms for segmentation of scar tissue from late gadolinium enhancement cardiovascular magnetic resonance of the left atrium: an open-access grand challenge. J. Cardiovasc. Magn. Reson 15, 105.
Kerckhoffs, R.C.P., Lumens, J., Vernooy, K., et al., 2008. Cardiac resynchronization: insight from experimental and computational models. Prog. Biophys. Mol. Biol. 97, 543–561.
Kerfoot, E., Lamata, P., Niederer, S., et al., 2013. Share and enjoy: anatomical models database–generating and sharing cardiovascular model data using web services. Med. Biol. Eng. Comput. 51, 1181–1190. http://dx.doi.org/10.1007/s11517-012-1023-4.
Kim, D.-H., Lu, N., Ghaffari, R., et al., 2011. Materials for multifunctional balloon catheters with capabilities in cardiac electrophysiological mapping and ablation therapy. Nat. Mater. 10, 316–323.
Kim, Y.H., Xie, F., Yashima, M., et al., 1999. Role of papillary muscle in the generation and maintenance of reentry during ventricular tachycardia and fibrillation in isolated swine right ventricle. Circulation 100, 1450–1459.
Knackstedt, C., Schauerte, P., Kirchhof, P., 2008. Electro-anatomic mapping systems in arrhythmias. Europace 10 (Suppl. 3), iii28–34.
Kohl, P., Bollensdorff, C., Garny, A., 2006. Effects of mechanosensitive ion channels on ventricular electrophysiology: experimental and theoretical models. Exp. Physiol. 91, 307–321.
Kohl, P., Crampin, E.J., Quinn, T.A., Noble, D., 2010. Systems biology: an approach. Clin. Pharmacol. Ther. 88, 25–33.
Kohl, P., Hunter, P., Noble, D., 1999. Stretch-induced changes in heart rate and rhythm: clinical observations, experiments and mathematical models. Prog. Biophys. Mol. Biol. 71, 91–138.
Kohl, P., Noble, D., 2009. Systems biology and the virtual physiological human. Mol. Syst. Biol. 5, 292. http://dx.doi.org/10.1038/msb.2009.51.
Konofagou, E.E., Provost, J., 2012. Electromechanical wave imaging for noninvasive mapping of the 3D electrical activation sequence in canines and humans in vivo. J. Biomech. 45, 856–864.
Krishnamurthy, A., Villongco, C.T., Chuang, J., et al., 2013. Patient-specific models of cardiac biomechanics. J. Comput. Phys. 244, 4–21.
Krittian, S.B.S., Lamata, P., Michler, C., et al., 2012. A finite-element approach to the direct computation of relative cardiovascular pressure from time-resolved MR velocity data. Med. Image Anal. 16, 1029–1037. http://dx.doi.org/10.1016/j.media.2012.04.003.
Lafortune, P., Arís, R., Vázquez, M., Houzeaux, G., 2012. Coupled electromechanical model of the heart: parallel finite element formulation. Int. J. Numer. Method Biomed. Eng. 28, 72–86.
Lamata, P., Niederer, S., Nordsletten, D., et al., 2011. An accurate, fast and robust method to generate patient-specific cubic Hermite meshes. Med. Image Anal. 15, 801–813. http://dx.doi.org/10.1016/j.media.2011.06.010.
Lamata, P., Lazdam, M., Ashcroft, A., et al., 2013a. Computational mesh as a descriptor of left ventricular shape for clinical diagnosis. Comput. Cardiol. 40, 571–574, 6713441.
Lamata, P., Pitcher, A., Krittian, S., et al., 2013b. Aortic relative pressure components derived from four-dimensional flow cardiovascular magnetic resonance. Magn. Reson. Med. http://dx.doi.org/10.1002/mrm.25015.
Lamata, P., Roy, I., Blazevic, B., et al., 2013c. Quality metrics for high order meshes: analysis of the mechanical simulation of the heart beat. IEEE Trans. Med. Imaging 32, 130–138. http://dx.doi.org/10.1109/TMI.2012.2231094.
Lamata, P., Sinclair, M., Kerfoot, E., et al., 2014. An automatic service for the personalization of ventricular cardiac meshes. J. R. Soc. Interface 11, 20131023. http://dx.doi.org/10.1098/rsif.2013.1023.
Lang, R.M., Badano, L.P., Tsang, W., et al., 2012. EAE/ASE recommendations for image acquisition and display using three-dimensional echocardiography. Eur. Heart J. Cardiovasc Imaging 13, 1–46. http://dx.doi.org/10.1093/ehjci/jer316.
Laughner, J.I., Ng, F.S., Sulkin, M.S., et al., 2012. Processing and analysis of cardiac optical mapping data obtained with potentiometric dyes. Am. J. Physiol. Heart Circ. Physiol. 303, H753–H765.
Ledesma-Carbayo, M.J., Kybic, J., Desco, M., et al., 2005. Spatio-temporal nonrigid registration for ultrasound cardiac motion estimation. IEEE Trans. Med. Imaging 24, 1113–1126.
Lee, G., Kumar, S., Teh, A., et al., 2014. Epicardial wave mapping in human long-lasting persistent atrial fibrillation: transient rotational circuits, complex wavefronts, and disorganized activity. Eur. Heart J. 35, 86–97.
Lee, J., Smith, N.P., 2012. The multi-scale modelling of coronary blood flow. Ann. Biomed. Eng. 40, 2399–2413.

Leenders, G.E., Lumens, J., Cramer, M.J., et al., 2012. Septal deformation patterns delineate mechanical dyssynchrony and regional differences in contractility: analysis of patient data using a computer model. Circ. Heart Fail 5, 87–96.
Legrice, I.J., Hunter, P.J., Smaill, B.H., 1997. Laminar structure of the heart: a mathematical model. Am. J. Physiol. 272, H2466–H2476.
LeGrice, I.J., Smaill, B.H., Chai, L.Z., et al., 1995. Laminar structure of the heart: ventricular myocyte arrangement and connective tissue architecture in the dog. Am. J. Physiol. 269, H571–H582.
Lewandowski, A.J., Augustine, D., Lamata, P., et al., 2013. Preterm heart in adult life: cardiovascular magnetic resonance reveals distinct differences in left ventricular mass, geometry, and function. Circulation 127, 197–206. http://dx.doi.org/10.1161/CIRCULATIONAHA.112.126920.
Li, J., Greener, I.D., Inada, S., et al., 2008. Computer three-dimensional reconstruction of the atrioventricular node. Circ. Res. 102, 975–985. http://dx.doi.org/10.1161/CIRCRESAHA.108.172403.
Li, P., Rudy, Y., 2011. A model of canine purkinje cell electrophysiology and Ca(2+) cycling: rate dependence, triggered activity, and comparison to ventricular myocytes. Circ. Res. 109, 71–79.
Li, W., Kohl, P., Trayanova, N., 2004. Induction of ventricular arrhythmias following mechanical impact: a simulation study in 3D. J. Mol. Histol. 35, 679–686.
Lloyd, C.M., Halstead, M.D.B., Nielsen, P.F., 2004. CellML: its future, present and past. Prog. Biophys. Mol. Biol. 85, 433–450.
Lohezic, M., Teh, I., Bollensdorff, C., Peyronnet, R., Hales, P., Grau, V., Kohl, P., Schneider, J., 2014. Interrogation of living myocardium in multiple static deformation states with diffusion tensor and diffusion spectrum imaging. Prog Bio Mol Biol 115 (2-3), 213–225. http://dx.doi.org/10.1016/j.pbiomolbio.2014.08.002.
Lombaert, H., Peyrat, J.-M., Croisille, P., et al., 2012. Human atlas of the cardiac fiber architecture: study on a healthy population. IEEE Trans. Med. Imaging 31, 1436–1447.
Lumens, J., Leenders, G.E., Cramer, M.J., et al., 2012. Mechanistic evaluation of echocardiographic dyssynchrony indices: patient data combined with multiscale computer simulations. Circ. Cardiovasc Imaging 5, 491–499.
Lumens, J., Ploux, S., Strik, M., et al., 2013. Comparative electromechanical and hemodynamic effects of left ventricular and biventricular pacing in dyssynchronous heart failure: electrical resynchronization versus left-right ventricular interaction. J. Am. Coll. Cardiol. 62, 2395–2403.
Luther, S., Fenton, F.H., Kornreich, B.G., et al., 2011. Low-energy control of electrical turbulence in the heart. Nature 475, 235–239.
MacLeod, R.S., Stinstra, J.G., Lew, S., et al., 2009. Subject-specific, multiscale simulation of electrophysiology: a software pipeline for image-based models and application examples. Philos. Trans. A Math. Phys. Eng. Sci. 367, 2293–2310.
Maesen, B., Zeemering, S., Afonso, C., et al., 2013. Rearrangement of atrial bundle architecture and consequent changes in anisotropy of conduction constitute the 3-dimensional substrate for atrial fibrillation. Circ. Arrhythm. Electrophysiol. 6, 967–975.
Markl, M., Kilner, P.J., Ebbers, T., 2011. Comprehensive 4D velocity mapping of the heart and great vessels by cardiovascular magnetic resonance. J. Cardiovasc Magn. Reson 13, 7.
Massé, S., Downar, E., Chauhan, V., et al., 2007. Ventricular fibrillation in myopathic human hearts: mechanistic insights from in vivo global endocardial and epicardial mapping. Am. J. Physiol. Heart Circ. Physiol. 292, H2589–H2597. http://dx.doi.org/10.1152/ajpheart.01336.2006.
McCormick, M., Nordsletten, D., Lamata, P., Smith, N.P., 2014. Computational analysis of the importance of flow synchrony for cardiac ventricular assist devices. Comput. Biol. Med. 49, 83–94. http://dx.doi.org/10.1016/j.compbiomed.2014.03.013.
McDowell, K.S., Arevalo, H.J., Maleckar, M.M., Trayanova, N.A., 2011. Susceptibility to arrhythmia in the infarcted heart depends on myofibroblast density. Biophys. J. 101, 1307–1315.
McDowell, K.S., Vadakkumpadan, F., Blake, R., et al., 2012. Methodology for patient-specific modeling of atrial fibrosis as a substrate for atrial fibrillation. J. Electrocardiol. 45, 640–645.
McDowell, K.S., Vadakkumpadan, F., Blake, R., et al., 2013. Mechanistic inquiry into the role of tissue remodeling in fibrotic lesions in human atrial fibrillation. Biophys. J. 104, 2764–2773.
Medrano-Gracia, P., Cowan, B.R., Bluemke, D.A., et al., 2013. Atlas-based analysis of cardiac shape and function: correction of regional shape bias due to imaging protocol for population studies. J. Cardiovasc Magn. Reson 15, 80.
Mondillo, S., Galderisi, M., Mele, D., et al., 2011. Speckle-tracking echocardiography: a new technique for assessing myocardial function. J. Ultrasound Med. 30, 71–83.
Moreno, J.D., Zhu, Z.I., Yang, P.-C., et al., 2011. A computational model to predict the effects of class I anti-arrhythmic drugs on ventricular rhythms. Sci. Transl. Med. 3, 98ra83.
Nademanee, K., McKenzie, J., Kosar, E., et al., 2004. A new approach for catheter ablation of atrial fibrillation: mapping of the electrophysiologic substrate. J. Am. Coll. Cardiol. 43, 2044–2053. http://dx.doi.org/10.1016/j.jacc.2003.12.054.
Nash, M.P., Bradley, C.P., Sutton, P.M., et al., 2006. Whole heart action potential duration restitution properties in cardiac patients: a combined clinical and modelling study. Exp. Physiol. 91, 339–354.
Nash, M.P., Hunter, P.J., 2000. Computational mechanics of the heart. J. Elast. Phys. Sci. Solids 61, 113–141.
Ng, J.J.K., Jacobson, J.T., Gordon, D., et al., 2012. Virtual electrophysiological study in a 3-dimensional cardiac magnetic resonance imaging model of porcine myocardial infarction. J. Am. Coll. Cardiol. 60, 423–430. http://dx.doi.org/10.1016/j.jacc.2012.03.029.
Niederer, S.A., Lamata, P., Plank, G., et al., 2012a. Analyses of the redistribution of work following cardiac resynchronisation therapy in a patient specific model. PLoS One 7, e43504. http://dx.doi.org/10.1371/journal.pone.0043504.
Niederer, S.A., Plank, G., Chinchapatnam, P., et al., 2011. Length-dependent tension in the failing heart and the efficacy of cardiac resynchronization therapy. Cardiovasc. Res. 89, 336–343. http://dx.doi.org/10.1093/cvr/cvq318.
Niederer, S.A., Shetty, A.K., Plank, G., et al., 2012b. Biophysical modeling to simulate the response to multisite left ventricular stimulation using a quadripolar pacing lead. Pacing Clin. Electrophysiol. 35, 204–214.
Nielles-Vallespin, S., Mekkaoui, C., Gatehouse, P., et al., 2013. In vivo diffusion tensor MRI of the human heart: reproducibility of breath-hold and navigator-based approaches. Magn. Reson Med. 70, 454–465. http://dx.doi.org/10.1002/mrm.24488.
Nielsen, P.M., Le Grice, I.J., Smaill, B.H., Hunter, P.J., 1991. Mathematical model of geometry and fibrous structure of the heart. Am. J. Physiol. 260, H1365–H1378.
Nielsen, T.D., Huang, J., Rogers, J.M., et al., 2009. Epicardial mapping of ventricular fibrillation over the posterior descending artery and left posterior papillary muscle of the swine heart. J. Interv. Card. Electrophysiol. 24, 11–17.
Noble, D., 1962. A modification of the Hodgkin–Huxley equations applicable to Purkinje fibre action and pace-maker potentials. J. Physiol. 160, 317–352.
Noble, D., 1960. Cardiac action and pacemaker potentials based on the Hodgkin-Huxley equations. Nature 188, 495–497. http://dx.doi.org/10.1038/188495b0.
Noble, D., 2011. Successes and failures in modeling heart cell electrophysiology. Heart Rhythm 8, 1798–1803.
Nordsletten, D.A., Niederer, S.A., Nash, M.P., et al., 2011. Coupling multi-physics models to cardiac mechanics. Prog. Biophys. Mol. Biol. 104 (1-3), 77–88.
Noujaim, S.F., Berenfeld, O., Kalifa, J., et al., 2007. Universal scaling law of electrical turbulence in the mammalian heart. Proc. Natl. Acad. Sci. U. S. A. 104, 20985–20989. http://dx.doi.org/10.1073/pnas.0709758104.
O'Hara, T., Rudy, Y., 2012. Quantitative comparison of cardiac ventricular myocyte electrophysiology and response to drugs in human and nonhuman species. Am. J. Physiol. Heart Circ. Physiol. 302, H1023–H1030.
Oakes, R.S., Badger, T.J., Kholmovski, E.G., et al., 2009. Detection and quantification of left atrial structural remodeling with delayed-enhancement magnetic resonance imaging in patients with atrial fibrillation. Circulation 119, 1758–1767.
Odening, K.E., Jung, B.A., Lang, C.N., et al., 2013. Spatial correlation of action potential duration and diastolic dysfunction in transgenic and drug-induced LQT2 rabbits. Heart Rhythm 10, 1533–1541.
Okada, J.-I., Washio, T., Maehara, A., et al., 2011. Transmural and apicobasal gradients in repolarization contribute to T-wave genesis in human surface ECG. Am. J. Physiol. Heart Circ. Physiol. 301, H200–H208. http://dx.doi.org/10.1152/ajpheart.01241.2010.
Pedrizzetti, G., La Canna, G., Alfieri, O., Tonti, G., 2014. The vortex-an early predictor of cardiovascular outcome? Nat. Rev. Cardiol. http://dx.doi.org/10.1038/nrcardio.2014.75.
Peebles, C., 2013. The year in cardiology 2012: imaging, computed tomography, and cardiovascular magnetic resonance. Eur. Heart J. 34, 310–313. http://dx.doi.org/10.1093/eurheartj/ehs406.
Pennell, D.J., Sechtem, U.P., Higgins, C.B., et al., 2004. Clinical indications for cardiovascular magnetic resonance (CMR): consensus panel report. Eur. Heart J. 25, 1940–1965. http://dx.doi.org/10.1016/j.ehj.2004.06.040.
Pertsov, A.M., Davidenko, J.M., Salomonsz, R., et al., 1993. Spiral waves of excitation underlie reentrant activity in isolated cardiac muscle. Circ. Res. 72, 631–650.
Petersen, S.E., Matthews, P.M., Bamberg, F., et al., 2013. Imaging in population science: cardiovascular magnetic resonance in 100,000 participants of UK Biobank – rationale, challenges and approaches. J. Cardiovasc Magn. Reson 15, 46.
Pitt-Francis, J., Garny, A., Gavaghan, D., 2006. Enabling computer models of the heart for high-performance computers and the grid. Philos. Trans. A Math. Phys. Eng. Sci. 364, 1501–1516.
Plank, G., Burton, R.A.B., Hales, P., et al., 2009. Generation of histo-anatomically representative models of the individual heart: tools and application. Philos. Trans. A Math. Phys. Eng. Sci. 367, 2257–2292.
Poon, M., Fuster, V., Fayad, Z., 2002. Cardiac magnetic resonance imaging: a "one-stop-shop" evaluation of myocardial dysfunction. Curr. Opin. Cardiol. 17, 663–670.
Pope, A.J., Sands, G.B., Smaill, B.H., LeGrice, I.J., 2008. Three-dimensional transmural organization of perimysial collagen in the heart. Am. J. Physiol. Heart Circ. Physiol. 295, H1243–H1252.
Prakosa, A., Malamas, P., Zhang, S., Pashakhanloo, F., Arevalo, H., Herzka, D.A., Lardo, A., Halperin, H., McVeigh, E., Trayanova, N., Vadakkumpadan, F., 2014. Methodology for image-based reconstruction of ventricular geometry for patient-specific modeling of cardiac electrophysiology. Prog Bio Mol Biol 115 (2-3), 226–234. http://dx.doi.org/10.1016/j.pbiomolbio.2014.08.009.
Provost, J., Gambhir, A., Vest, J., et al., 2013. A clinical feasibility study of atrial and ventricular electromechanical wave imaging. Heart Rhythm 10, 856–862.
Provost, J., Gurev, V., Trayanova, N., Konofagou, E.E., 2011a. Mapping of cardiac electrical activation with electromechanical wave imaging: an in silico-in vivo reciprocity study. Heart Rhythm 8, 752–759.
Provost, J., Lee, W.-N., Fujikura, K., Konofagou, E.E., 2011b. Imaging the electromechanical activity of the heart in vivo. Proc. Natl. Acad. Sci. U. S. A. 108, 8565–8570.
Quinn, T.A., Granite, S., Allessie, M.A., et al., 2011. Minimum information about a cardiac electrophysiology Experiment (MICEE): standardised reporting for

model reproducibility, interoperability, and data sharing. Prog. Biophys. Mol. Biol. 107, 4–10.
Quinn, T.A., Kohl, P., 2013. Combining wet and dry research: experience with model development for cardiac mechano-electric structure-function studies. Cardiovasc Res. 97, 601–611.
Ramanathan, C., Ghanem, R.N., Jia, P., et al., 2004. Noninvasive electrocardiographic imaging for cardiac electrophysiology and arrhythmia. Nat. Med. 10, 422–428.
Ranjan, R., Kholmovski, E.G., Blauer, J., et al., 2012. Identification and acute targeting of gaps in atrial ablation lesion sets using a real-time magnetic resonance imaging system. Circ. Arrhythm. Electrophysiol. 5, 1130–1135.
Rantner, L.J., Arevalo, H.J., Constantino, J.L., et al., 2012. Three-dimensional mechanisms of increased vulnerability to electric shocks in myocardial infarction: altered virtual electrode polarizations and conduction delay in the peri-infarct zone. J. Physiol. 590, 4537–4551.
Rantner, L.J., Tice, B.M., Trayanova, N.A., 2013a. Terminating ventricular tachyarrhythmias using far-field low-voltage stimuli: mechanisms and delivery protocols. Heart Rhythm 10, 1209–1217.
Rantner, L.J., Vadakkumpadan, F., Spevak, P.J., et al., 2013b. Placement of implantable cardioverter-defibrillators in paediatric and congenital heart defect patients: a pipeline for model generation and simulation prediction of optimal configurations. J. Physiol. 591, 4321–4334.
Relan, J., Pop, M., Delingette, H., et al., 2011. Personalization of a cardiac electrophysiology model using optical mapping and MRI for prediction of changes with pacing. IEEE Trans. Biomed. Eng. 58, 3339–3349.
Robert, B., Sinkus, R., Gennisson, J.-L., Fink, M., 2009. Application of DENSE-MR-elastography to the human heart. Magn. Reson Med. 62, 1155–1163.
Rodriguez, B., Burrage, K., Gavaghan, D., et al., 2010. The systems biology approach to drug development: application to toxicity assessment of cardiac drugs. Clin. Pharmacol. Ther. 88, 130–134.
Rodríguez, B., Li, L., Eason, J.C., et al., 2005. Differences between left and right ventricular chamber geometry affect cardiac vulnerability to electric shocks. Circ. Res. 97, 168–175.
Romero, D., Sebastian, R., Bijnens, B.H., et al., 2010. Effects of the purkinje system and cardiac geometry on biventricular pacing: a model study. Ann. Biomed. Eng. 38, 1388–1398.
Sands, G., Goo, S., Gerneke, D., et al., 2011. The collagenous microstructure of cardiac ventricular trabeculae carneae. J. Struct. Biol. 173, 110–116.
Schuster, A., Chiribiri, A., Ishida, M., et al., 2012. Cardiovascular magnetic resonance imaging of isolated perfused pig hearts in a 3T clinical MR scanner. Interv. Med. Appl. Sci. 4, 186–192.
Scollan, D.F., Holmes, A., Winslow, R., Forder, J., 1998. Histological validation of myocardial microstructure obtained from diffusion tensor magnetic resonance imaging. Am. J. Physiol. 275, H2308–H2318.
Sermesant, M., Chabiniok, R., Chinchapatnam, P., et al., 2012. Patient-specific electromechanical models of the heart for the prediction of pacing acute effects in CRT: a preliminary clinical validation. Med. Image Anal. 16, 201–215.
Sermesant, M., Delingette, H., Ayache, N., 2006a. An electromechanical model of the heart for image analysis and simulation. IEEE Trans. Med. Imaging 25, 612–625.
Sermesant, M., Moireau, P., Camara, O., et al., 2006b. Cardiac function estimation from MRI using a heart model and data assimilation: advances and difficulties. Med. Image Anal. 10, 642–656.
Silva, J.N.A., Ghosh, S., Bowman, T.M., et al., 2009. Cardiac resynchronization therapy in pediatric congenital heart disease: insights from noninvasive electrocardiographic imaging. Heart Rhythm 6, 1178–1185.
Simpson, R.M., Keegan, J., Firmin, D.N., 2013. MR assessment of regional myocardial mechanics. J. Magn. Reson. Imaging 37, 576–599.
Solovyova, O., Katsnelson, L.B., Konovalov, P., et al., 2006. Activation sequence as a key factor in spatio-temporal optimization of myocardial function. Philos. Trans. A Math. Phys. Eng. Sci. 364, 1367–1383.
Solovyova, O., Katsnelson, L.B., Konovalov, P.V., Kursanov, A.G., Vikulova, N.A., Kohl, P., Markhasin, V.S., 2014. The cardiac muscle duplex as a method to study myocardial heterogeneity. Prog Biophys Mol Biol 115 (2-3), 114–127. http://dx.doi.org/10.1016/j.pbiomolbio.2014.07.010.
Sosnovik, D.E., Mekkaoui, C., Huang, S., et al., 2014. Microstructural impact of ischemia and bone marrow-derived cell therapy revealed with diffusion tensor magnetic resonance imaging tractography of the heart in vivo. Circulation 129, 1731–1741.
Sosnovik, D.E., Wang, R., Dai, G., et al., 2009. Diffusion MR tractography of the heart. J. Cardiovasc Magn. Reson 11, 47. http://dx.doi.org/10.1186/1532-429X-11-47.
Spotnitz, H., 1974. Cellular basis for volume related wall thickness changes in the rat left ventricle. J. Mol. Cell. Cardiol. 6, 317–322.
Spotnitz, H.M., 2000. Macro design, structure, and mechanics of the left ventricle. J. Thorac. Cardiovasc. Surg. 119, 1053–1077.
Taegtmeyer, H., Dilsizian, V., 2013. Imaging cardiac metabolism. In: Dilsizian, V., Narula, J. (Eds.), Atlas Nucl. Cardiol, fourth ed. Springer, pp. 289–321.
Taggart, P., Sutton, P., Opthof, T., et al., 2003. Electrotonic cancellation of transmural electrical gradients in the left ventricle in man. Prog. Biophys. Mol. Biol. 82, 243–254.
Taylor, C.A., Figueroa, C.A., 2009. Patient-specific modeling of cardiovascular mechanics. Annu Rev. Biomed. Eng. 11, 109–134.
Taylor, C.A., Fonte, T.A., Min, J.K., 2013. Computational fluid dynamics applied to cardiac computed tomography for noninvasive quantification of fractional flow reserve: scientific basis. J. Am. Coll. Cardiol. 61, 2233–2241.
Ten Tusscher, K.H.W.J., Mourad, A., Nash, M.P., et al., 2009. Organization of ventricular fibrillation in the human heart: experiments and models. Exp. Physiol. 94, 553–562.
Ten Tusscher, K.H.W.J., Panfilov, A.V., 2008. Modelling of the ventricular conduction system. Prog. Biophys. Mol. Biol. 96, 152–170.
Thompson, P.M., Mega, M.S., Narr, K.L., et al., 2000. Brain Image Analysis and Atlas Construction. In: Handb Med Imaging, vol. 2. http://dx.doi.org/10.1117/3.831079.ch17.
Toussaint, N., Stoeck, C.T., Schaeffter, T., et al., 2013. In vivo human cardiac fibre architecture estimation using shape-based diffusion tensor processing. Med. Image Anal. 17, 1243–1255.
Townsend, D.W., 2008. Multimodality imaging of structure and function. Phys. Med. Biol. 53, R1–R39.
Trayanova, N.A., 2011. Whole-heart modeling: applications to cardiac electrophysiology and electromechanics. Circ. Res. 108, 113–128. http://dx.doi.org/10.1161/CIRCRESAHA.110.223610.
Trayanova, N.A., 2014. Mathematical approaches to understanding and imaging atrial fibrillation: significance for mechanisms and management. Circ. Res. 114, 1516–1531.
Vadakkumpadan, F., Arevalo, H., Prassl, A.J., et al., 2010. Image-based models of cardiac structure in health and disease. Wiley Interdiscip. Rev. Syst. Biol. Med. 2, 489–506.
Vadakkumpadan, F., Rantner, L.J., Tice, B., et al., 2009. Image-based models of cardiac structure with applications in arrhythmia and defibrillation studies. J. Electrocardiol. 42, 157.e1-10.
Valderrábano, M., Chen, P.-S., Lin, S.-F., 2003. Spatial distribution of phase singularities in ventricular fibrillation. Circulation 108, 354–359.
Valderrábano, M., Lee, M.H., Ohara, T., et al., 2001. Dynamics of intramural and transmural reentry during ventricular fibrillation in isolated swine ventricles. Circ. Res. 88, 839–848.
Vaquero, M., Calvo, D., Jalife, J., 2008. Cardiac fibrillation: from ion channels to rotors in the human heart. Heart Rhythm 5, 872–879.
Vatasescu, R., Berruezo, A., Mont, L., et al., 2009. Midterm "super-response" to cardiac resynchronization therapy by biventricular pacing with fusion: insights from electro-anatomical mapping. Europace 11, 1675–1682.
Vigmond, E.J., Clements, C., 2007. Construction of a computer model to investigate sawtooth effects in the Purkinje system. IEEE Trans. Biomed. Eng. 54, 389–399.
Waldman, L.K., Nosan, D., Villarreal, F., Covell, J.W., 1988. Relation between transmural deformation and local myofiber direction in canine left ventricle. Circ. Res. 63, 550–562.
Wang, H., Amini, A.A., 2012. Cardiac motion and deformation recovery from MRI: a review. IEEE Trans. Med. Imaging 31, 487–503.
Wang, V.Y., Lam, H.I., Ennis, D.B., et al., 2009. Modelling passive diastolic mechanics with quantitative MRI of cardiac structure and function. Med. Image Anal. 13, 773–784.
Weber, K.T., Sun, Y., Tyagi, S.C., Cleutjens, J.P., 1994. Collagen network of the myocardium: function, structural remodeling and regulatory mechanisms. J. Mol. Cell. Cardiol. 26, 279–292.
Wilkoff, B.L., Bello, D., Taborsky, M., et al., 2011. Magnetic resonance imaging in patients with a pacemaker system designed for the magnetic resonance environment. Heart Rhythm 8, 65–73.
Winslow, R.L., Tanskanen, A., Chen, M., Greenstein, J.L., 2006. Multiscale modeling of calcium signaling in the cardiac dyad. Ann. N. Y. Acad. Sci. 1080, 362–375.
Wong, J., Baddeley, D., Bushong, E.A., et al., 2013. Nanoscale distribution of ryanodine receptors and caveolin-3 in mouse ventricular myocytes: dilation of t-tubules near junctions. Biophys. J. 104, L22–L24.
Xi, J., Lamata, P., Lee, J., et al., 2011. Myocardial transversely isotropic material parameter estimation from in-silico measurements based on a reduced-order unscented Kalman filter. J. Mech. Behav. Biomed. Mater. 4, 1090–1102. http://dx.doi.org/10.1016/j.jmbbm.2011.03.018.
Xi, J., Lamata, P., Niederer, S., et al., 2013. The estimation of patient-specific cardiac diastolic functions from clinical measurements. Med. Image Anal. 17, 133–146. http://dx.doi.org/10.1016/j.media.2012.08.001.
Xi, J., Shi, W., Rueckert, D., et al., 2014. Understanding the need of ventricular pressure for the estimation of diastolic biomarkers. Biomech. Model Mechanobiol. 13, 747–757. http://dx.doi.org/10.1007/s10237-013-0531-y.
Xie, Y., Garfinkel, A., Camelliti, P., et al., 2009. Effects of fibroblast-myocyte coupling on cardiac conduction and vulnerability to reentry: a computational study. Heart Rhythm 6, 1641–1649.
Xu, L., Gutbrod, S.R., Bonifas, A.P., et al., 2014. 3D multifunctional integumentary membranes for spatiotemporal cardiac measurements and stimulation across the entire epicardium. Nat. Commun. 5, 3329.
Yotti, R., Bermejo, J., Benito, Y., et al., 2011. Noninvasive estimation of the rate of relaxation by the analysis of intraventricular pressure gradients. Circ. Cardiovasc Imaging 4, 94–104.
Young, A.A., Frangi, A.F., 2009. Computational cardiac atlases: from patient to population and back. Exp. Physiol. 94, 578–596.
Zemzemi, N., Bernabeu, M.O., Saiz, J., et al., 2013. Computational assessment of drug-induced effects on the electrocardiogram: from ion channel to body surface potentials. Br. J. Pharmacol. 168, 718–733.
Zhang, H., Holden, A.V., Kodama, I., et al., 2000. Mathematical models of action potentials in the periphery and center of the rabbit sinoatrial node. Am. J. Physiol. Heart Circ. Physiol. 279, H397–H421.